

# Pairwise Weights for Temporal Credit Assignment

Zeyu Zheng<sup>1\*</sup> Risto Vuorio<sup>1\*†</sup> Richard Lewis<sup>1</sup> Satinder Singh<sup>1</sup>

## Abstract

How much credit (or blame) should an action taken in a state get for a future reward? This is the fundamental temporal credit assignment problem in Reinforcement Learning (RL). One of the earliest and still most widely used heuristics is to assign this credit based on a scalar coefficient  $\lambda$  (treated as a hyperparameter) raised to the power of the time interval between the state-action and the reward. In this empirical paper, we explore heuristics based on more general pairwise weightings that are functions of the state in which the action was taken, the state at the time of the reward, as well as the time interval between the two. Of course it isn't clear what these pairwise weight functions should be, and because they are too complex to be treated as hyperparameters we develop a metagradient procedure for learning these weight functions during the usual RL training of a policy. Our empirical work shows that it is often possible to learn these pairwise weight functions during learning of the policy to achieve better performance than competing approaches.

## 1. Introduction

The following *umbrella problem* (Osband et al., 2019) illustrates a fundamental challenge in most reinforcement learning (RL) problems, namely the *temporal credit assignment* (TCA) problem. An RL agent takes an umbrella at the start of a cloudy workday morning and experiences a long day at work filled with various rewards uninfluenced by the umbrella, before needing the umbrella in the rain on the way home. The agent must learn to credit the take-umbrella action in the cloudy-morning state with the very delayed reward at the end of the day, while also learning to not credit the action with the many intervening rewards, despite their occurring much closer in time. More generally, the TCA

problem is how much credit or blame should an action taken in a state get for a future reward. One of the earliest and still most widely used heuristics for TCA assigns credit based on a scalar coefficient  $\lambda$  raised to the power of the time interval between the state-action and the reward. This heuristic comes from the celebrated TD( $0 \leq \lambda \leq 1$ ) (Sutton, 1988) family of algorithms and has since been adopted in most modern RL algorithms.

In this empirical paper, we explore new heuristics for TCA based on more general (than TD( $\lambda$ )) pairwise weightings that are functions of *the state in which the action was taken*, *the state at the time of the reward*, as well as *the time interval between the two*. Of course, it isn't clear what this pairwise weight function should be, and it is too complex to be treated as a hyperparameter (in contrast to the scalar  $\lambda$  which is typically set by searching over a small set of values). We develop a metagradient approach to learning the pairwise weight function at the same time as learning the policy parameters of the agent. Like most metagradient algorithms, our algorithm has two loops: an outer loop that periodically updates the pairwise weight function in order to optimize the usual RL loss (policy-gradient loss in our case), and an inner loop where the policy parameters are updated using the pairwise weight function set by the outer loop.

Thus, our main contributions in this paper are a new pairwise weight function for TCA and a metagradient algorithm to learn such a function. Our empirical work is geared towards answering two questions: (1) Are the more general pairwise weight functions we propose able to outperform the best choice of  $\lambda$  as well as other baselines? and (2) Is our metagradient algorithm able to learn the pairwise weight functions fast enough to be worth the more complex learning problem they introduce?

**Related Work on Credit Assignment.** Several heuristic methods have been proposed to address the long-term credit assignment problem in RL. Hindsight Credit Assignment (HCA) (Harutyunyan et al., 2019) proposes the notion of hindsight return which leads to a new family of RL algorithms. Theoretically HCA can address some problems where classic RL algorithms struggle, e.g., counterfactual credit assignment. RUDDER (Arjona-Medina et al., 2019) trains a LSTM (Hochreiter & Schmidhuber, 1997) to predict the return of an episode given the entire state and action

\*Equal contribution †Now at the University of Oxford.

<sup>1</sup>University of Michigan. Correspondence to: Zeyu Zheng <zeyu@umich.edu>, Risto Vuorio <risto.vuorio@cs.ox.ac.uk>.

sequence. Then it conducts contribution analysis with the LSTM to decompose the return and redistribute rewards to state-action pairs. Temporal Value Transport (TVT) (Hung et al., 2019) augments the agent with an external memory module and utilizes the memory retrieval as a proxy for transporting future value back to related state-action pairs. Both RUDDER and TVT employ memory modules to identify key events in the trajectory to facilitate long-term credit assignment. We compare directly against TVT because their code was available and applicable, and we take inspiration from the core reward-redistribution idea from RUDDER and implement it within our policy gradient agent as a comparison baseline (because the available RUDDER code is not directly applicable). We do not compare against HCA because it is mainly a theoretical idea at this point and it is unclear how to implement it in a scalable way within DeepRL architectures. We also compare against two other algorithms that are more closely related to ours in their use of metagradients. Xu et al. (2018) adapt  $\lambda$  via metagradients rather than tuning it via hyperparameter search, thereby improving over the use of a fixed- $\lambda$  algorithm. The Return Generating Model (RGM) (Wang et al., 2019) generalizes the notion of return from exponentially discounted sum of rewards to a more flexibly weighted sum of rewards where the weights are adapted via metagradients during policy learning. RGM takes the entire episode as input and generates one weight for each time step. In contrast, we study pairwise weights as explained below.

## 2. Pairwise Weights for Advantages

At the core of our contribution are new parameterizations of functions for computing advantages used in policy gradient algorithms. Next, we briefly review advantages in policy gradient RL and TD( $\lambda$ ) as our points of departure for the new parameterizations.

**Background on Policy Gradient RL, Advantages, and TD( $\lambda$ ).** We assume an episodic RL setting. The agent’s policy  $\pi_\theta$ , parameterized by  $\theta$ , maps a state  $S$  to a probability distribution over the actions. Within each episode, at time step  $t$ , the agent observes the current state  $S_t$ , takes an action  $A_t \sim \pi_\theta(\cdot|S_t)$ , and receives the reward  $R_{t+1}$ . The performance measure for the policy  $\pi_\theta$ , denoted by  $J(\theta)$ , is defined as the expected sum of the rewards when the agent behaves according to  $\pi_\theta$ , i.e.,

$$J^\pi(\theta) = \mathbb{E}_{S_0 \sim \nu, A_t \sim \pi_\theta(\cdot|S_t), S_{t+1} \sim P(\cdot|S_t, A_t)} \left[ \sum_{t=1}^T \gamma^{t-1} R_t \right],$$

where  $\nu$  is the probability distribution of the initial state,  $P$  is the transition dynamics,  $T$  is the length of an episode, and  $\gamma$  is the discount factor. For brevity, henceforth we will denote the expectation in the equation above by  $\mathbb{E}_\theta$  unless

further clarification is needed. The gradient of  $J(\theta)$  w.r.t the policy parameters  $\theta$  is (Sutton et al., 2000; Williams, 1992)

$$\nabla_\theta J^\pi(\theta) = \mathbb{E}_\theta \left[ (G_t - b(S_t)) \nabla_\theta \log \pi_\theta(A_t|S_t) \right], \quad (1)$$

where  $G_t = \sum_{t'=t+1}^T \gamma^{t'-t-1} R_{t'}$  denotes the return and  $b(S_t)$  is an arbitrary baseline function for variance reduction. Typically this baseline is the value function  $V^\pi(s) = \mathbb{E}_\theta[G_t|S_t = s]$ , and the resulting difference is called the advantage function

$$\Psi^\pi(s, a) = \mathbb{E}_\theta[G_t - V^\pi(s)|S_t = s, A_t = a]. \quad (2)$$

For brevity, we will omit the superscript  $\pi$  on  $V$  and  $\Psi$ .

Since the true value function  $V$  is usually unknown, an estimated value function  $v$  is used in place of  $V$  to provide an approximation, which leads to a Monte-Carlo (MC) estimation of  $\Psi^\pi$ :

$$\hat{\Psi}_t^{\text{MC}} = G_t - v(S_t), \quad (3)$$

where  $\hat{\Psi}_t^{\text{MC}}$  is short for  $\hat{\Psi}^{\text{MC}}(S_t, A_t)$ . However,  $\hat{\Psi}^{\text{MC}}$  usually suffers from high variance. To reduce variance, the estimated value function is used to estimate the return as in the TD( $\lambda$ ) algorithm using the eligibility trace parameter  $\lambda$ ; specifically the new form of the return, called  $\lambda$ -return is a weighted sum of  $n$ -step truncated corrected returns where the correction uses the estimated value function after  $n$ -steps. The corresponding  $\lambda$ -estimator is

$$\hat{\Psi}_t^{(\lambda)} = \sum_{t'=t+1}^T (\gamma\lambda)^{t'-t-1} \delta_{t'}, \quad (4)$$

where  $\delta_t = R_t + \gamma v(S_t) - v(S_{t-1})$  is the TD-error at time  $t$  (Schulman et al., 2015). Note that when  $\lambda = 1$ , it recovers the MC estimator:

$$\hat{\Psi}_t^{(1)} = \sum_{t'=t+1}^T \gamma^{t'-t-1} \delta_{t'} = G_t - v(S_t) = \hat{\Psi}_t^{\text{MC}}. \quad (5)$$

As noted above, the value for  $\lambda$  is usually manually tuned as a hyperparameter. Adjusting  $\lambda$  provides a way to tradeoff bias and variance in  $\hat{\Psi}^\lambda$  (this is absent in  $\hat{\Psi}^{\text{MC}}$ ). Below we present two new estimators that are analogous in this regard to  $\hat{\Psi}^\lambda$  and  $\hat{\Psi}^{\text{MC}}$ .

**Proposed Heuristic 1: Advantages via Pairwise Weighted Sum of TD-errors.** Our first new estimator, denoted PWTD for Pairwise Weighted TD-error, is a strict generalization of the  $\lambda$ -estimator above and is defined as follows:

$$\hat{\Psi}_{\eta,t}^{\text{PWTD}} = \sum_{t'=t+1}^T f_\eta(S_t, S_{t'}, t' - t) \delta_{t'}, \quad (6)$$

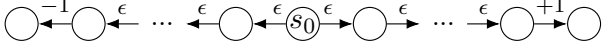


Figure 1. A simple MDP for illustration. The initial action in state  $s_0$  determines the reward for the last transition but does not influence the intermediate noisy rewards. The main consequence of the initial action is thus significantly delayed.

where  $f_\eta(S_t, S_{t'}, t' - t) \in [0, 1]$ , parameterized by  $\eta$ , is the weight given to the TD-error  $\delta_{t'}$  as a function of the state to which credit is being assigned, the state at which the TD-error is obtained, and the time interval between the two. Note that if we choose  $f$  to be  $f(S_t, S_{t'}, t' - t) = (\gamma\lambda)^{t' - t - 1}$ , it recovers the usual  $\lambda$ -estimator  $\hat{\Psi}^{(\lambda)}$ .

**Proposed Heuristic 2: Advantages via Pairwise Weighted Sum of Rewards.** Instead of generalizing from the  $\lambda$ -estimator, we can also generalize from the MC estimator via pairwise weighting. Specifically, the new pairwise-weighted return is defined as

$$G_{\eta,t}^{\text{PWR}} = \sum_{t'=t+1}^T f_\eta(S_t, S_{t'}, t' - t) R_{t'}, \quad (7)$$

where  $f_\eta(S_t, S_{t'}, t' - t) \in [0, 1]$  is the weight given to the reward  $R_{t'}$ . The corresponding advantage estimator, denoted PWR for **P**airwise **W**eighted **R**eward, then is:

$$\hat{\Psi}_{\eta,t}^{\text{PWR}} = G_{\eta,t}^{\text{PWR}} - v^{\text{PWR}}(S_t), \quad (8)$$

where  $V^{\text{PWR}}(s) = E_\theta[G_{\eta,t}^{\text{PWR}} | S_t = s]$  and  $v^{\text{PWR}}$  is an approximation of  $V^{\text{PWR}}$ . Note that if we choose  $f$  to be  $f(S_t, S_{t'}, t' - t) = \gamma^{t' - t - 1}$ , we can recover the MC estimator  $\hat{\Psi}^{\text{MC}}$ .

While the usual estimators  $\hat{\Psi}^{(\lambda)}$  and  $\hat{\Psi}^{\text{MC}}$  have some nice theoretical properties stemming from the guarantees associated with Monte-Carlo returns and  $\lambda$ -returns, we lose those guarantees for our generalizations  $\hat{\Psi}^{\text{PWR}}$  and  $\hat{\Psi}^{\text{PWRD}}$ . In particular, the new estimators can be unbounded in the infinite-horizon setting. However, this is less of a concern in practice because episodes are typically of finite expected length. Moreover, recall that these new estimators will be used in the inner loop of a metagradient algorithm and can thus be viewed as a flexible parameterization of advantages where the pairwise weight function is tuned from data using an outer loop that uses standard, theoretically justified, policy gradient losses. We will discuss this further in the next Section as well as validate the potential benefits in our empirical work. Next, we provide an illustrative example based on the umbrella problem (cf. §1) to show how exploiting the flexibility in the new estimators can be of benefit.

**An Illustrative Analysis of the Benefit of the PWR Estimator.** Consider the simple-MDP version of the Umbrella

problem in Figure 1. Each episode starts at the leftmost state,  $s_0$ , and consists of  $T$  transitions. The only choice of action is at  $s_0$  and it determines the reward on the last transition. A noisy reward  $\epsilon$  is sampled for each intermediate transition independently from a distribution with mean  $\mathbb{E}[\epsilon]$  and variance  $\text{Var}[\epsilon] > 0$ . By construction, the intermediate rewards are independent of the initial action. The expected return for state  $s_0$  under policy  $\pi$  is

$$V(s_0) = \mathbb{E}_\theta[G_0] = (T - 1)\mathbb{E}[\epsilon] + \mathbb{E}_{A_0 \sim \pi(\cdot | s_0)}[R_T].$$

For any initial action  $a_0$ , the advantage

$$\Psi(s_0, a_0) = \mathbb{E}_\epsilon[G_0 - V(s_0) | a_0] = \mathbb{E}_\epsilon\left[\sum_{i=1}^T R_i | a_0\right] - V(s_0) = \mathbb{E}[R_T | a_0] - \mathbb{E}_{A_0 \sim \pi(\cdot | s_0)}[R_T].$$

Consider pairwise weights for computing  $\hat{\Psi}^{\text{PWR}}(s_0, a_0)$  that place weight only on the final transition, and zero weight on the noisy intermediate rewards, capturing the notion that the intermediate rewards are not influenced by the initial action choice. More specifically, we choose  $f$  such that for any episode,  $w_{0T} = 1$  and  $w_{ij} = 0$  for other  $i$  and  $j$ . Here we use  $w_{ij}$  to denote  $f(S_i, S_j, j - i)$  for brevity. The expected parameterized reward sum for the initial state  $s_0$  is

$$V^{\text{PWR}}(s_0) = \mathbb{E}_\theta[G_{\eta,0}] = \mathbb{E}_\theta\left[\sum_{i=t}^T w_{0t} R_t\right] = \mathbb{E}_{A_0 \sim \pi(\cdot | s_0)}[R_T].$$

If  $v^{\text{PWR}}$  is correct, for any initial action  $a_0$ , the pairwise-weighted advantage is the same as the regular advantage:

$$\begin{aligned} \mathbb{E}_\epsilon[\hat{\Psi}_\eta^{\text{PWR}}(s_0, a_0)] &= \mathbb{E}_\epsilon[G_{\eta,0} - v^{\text{PWR}}(s_0) | a_0] \\ &= \mathbb{E}_\epsilon\left[\sum_{t=1}^T w_{0t} R_t\right] - V^{\text{PWR}}(s_0) \\ &= \mathbb{E}[R_T | a_0] - \mathbb{E}_{A_0 \sim \pi(\cdot | s_0)}[R_T] \\ &= \Psi(s_0, a_0). \end{aligned}$$

As for variance, for any initial action  $a_0$ ,  $[G_{\eta,0} | a_0]$  is deterministic because of the zero weight on all the intermediate rewards and thus  $\hat{\Psi}_\eta^{\text{PWR}}(s_0, a_0)$  has zero variance. The variance of  $\hat{\Psi}^{\text{MC}}(s_0, a_0)$  on the other hand is  $(T - 1)\text{Var}[\epsilon] > 0$ .

Thus, in this illustrative example  $\hat{\Psi}^{\text{PWR}}$  yields an unbiased advantage estimator with far lower variance than  $\hat{\Psi}^{\text{MC}}$ .

Our example exploited knowledge of the domain to set weights that would yield an unbiased advantage estimator with reduced variance, thereby providing some intuition on how a more flexible return might in principle yield benefits for learning. Of course, in general RL problems will have the Umbrella Problem in them to varying degrees. But how can these weights be set by the agent itself, without prior knowledge of the domain? We turn to this question next.

### 3. A Metagradient Algorithm for Adapting Pairwise Weights

Recently metagradient methods have been developed to learn various kinds of parameters that would otherwise be set by hand or by manual hyperparameter search; these include discount factors (Xu et al., 2018; Zahavy et al., 2020), intrinsic rewards (Zheng et al., 2018; Rajendran et al., 2019; Zheng et al., 2019), auxiliary tasks (Veeriah et al., 2019), constructing general return functions (Wang et al., 2019), and discovering new RL objectives (Oh et al., 2020; Xu et al., 2020). We develop a similar metagradient algorithm for learning pairwise weight functions during policy-gradient learning: an outer loop learner for the pairwise weight function is driven by a conventional policy gradient loss, while an inner loop learner is driven by a policy-gradient loss based on the new pairwise-weighted advantages. An overview of the algorithm is in the Supplement. In the rest of this section, we use a unified notation  $\hat{\Psi}_\eta$  to denote  $\hat{\Psi}_\eta^{\text{PWTD}}$  or  $\hat{\Psi}_\eta^{\text{PWR}}$  unless it causes ambiguity.

**Learning in the Inner Loop.** In the inner loop, the pairwise-weighted advantage  $\hat{\Psi}_\eta$  is used to compute the policy gradient. We rewrite the gradient update from Eq. 1 with the new advantage as

$$\nabla_\theta J_\eta^\pi(\theta) = \mathbb{E}_{\tau \sim \pi_\theta} \left[ \sum_{t=0}^{T-1} \hat{\Psi}_\eta(S_t, A_t) \nabla_\theta \log \pi_\theta(A_t | S_t) \right],$$

where  $\tau$  is a trajectory sampled by executing  $\pi_\theta$ . The overall update to  $\theta$  is

$$\nabla_\theta J^{\text{inner}}(\theta) = \nabla_\theta J_\eta^\pi(\theta) + \beta^{\mathcal{H}} \nabla_\theta J^{\mathcal{H}}(\pi_\theta), \quad (9)$$

where  $J^{\mathcal{H}}(\theta)$  is the usual entropy regularization term to encourage exploration, and  $\beta^{\mathcal{H}}$  is a mixing coefficient.

Computing  $\hat{\Psi}_\eta^{\text{PWR}}$  with Equation 8 requires a value function predicting the expected pairwise-weighted sums of rewards. We train the value function,  $v_\psi$  with parameters  $\psi$ , along with the policy by minimizing the mean squared error between its output  $v_\psi(S_t)$  and the pairwise-weighted sum of rewards  $G_{\eta,t}$ . The objective for training  $v_\psi$  is

$$J_\eta^v(\psi) = \mathbb{E}_{\tau \sim \pi_\theta} \left[ \sum_{t=0}^{T-1} \frac{1}{2} (G_{\eta,t} - v_\psi(S_t))^2 \right]. \quad (10)$$

Note that  $\hat{\Psi}_\eta^{\text{PWTD}}$  does not need this extra value function.

**Updating  $\eta$  via Metagradient in the Outer Loop.** To update  $\eta$ , the parameters of the pairwise weight functions, we need to compute the gradient of the usual policy loss w.r.t.  $\eta$  through the effect of  $\eta$  on the inner loop’s parameters  $\theta$ . Recall that  $\eta$  determines the update of  $\theta$  to a new  $\theta'$  as defined above. Therefore, by chain rule

$$\nabla_\eta J^{\text{outer}}(\eta) = \nabla_{\theta'} J^\pi(\theta') \nabla_\eta \theta'. \quad (11)$$

where,

$$\nabla_{\theta'} J^\pi(\theta') = \mathbb{E}_{\tau' \sim \pi_{\theta'}} \left[ \sum_{i=0}^{T-1} \Psi(S_i, A_i) \nabla_{\theta'} \log \pi_{\theta'}(A_i | S_i) \right]$$

where  $\tau'$  is another trajectory sampled by executing the updated policy  $\pi_{\theta'}$  and  $\Psi(S_t, A_t)$  is the regular advantage.

Note that we need two trajectories,  $\tau$  and  $\tau'$ , to make one update to the meta-parameters  $\eta$ . The policy parameters  $\theta$  are updated with Equation 9 after collecting trajectory  $\tau$ . The next trajectory  $\tau'$  is collected using the updated parameters  $\theta'$ . The  $\eta$ -parameters are updated on  $\tau'$ . In order to make more efficient use of the data, we follow (Xu et al., 2018) and reuse the second trajectory  $\tau'$  in the next iteration as the trajectory for updating  $\theta$ . *In practice we use modern auto-differentiation tools to compute Equation 11 without applying the chain rule explicitly.*

Computing the regular advantage,  $\Psi(S_t, A_t)$ , requires an estimated value function for the regular return. This value function is parameterized by  $\phi$  and updated to minimize the mean squared error analogously to Equation 10.

## 4. Experiments

We present three sets of experiments. The first set (§4.1) uses simple tabular MDPs that allow visualization of the pairwise weights learned by Meta-PWTD and -PWR. The results show that the metagradient adaptation both *increases* and *decreases* weights in a way that can be interpreted as reflecting explicit credit assignment and variance reduction. In the second set (§4.2) we test Meta-PWTD and -PWR with neural networks in a 2D pixel-based variant of the benchmark credit assignment task *Key-to-Door* (Hung et al., 2019). We show that Meta-PWTD and -PWR outperform several existing methods for directly addressing credit assignment, as well as TD( $\lambda$ ) methods, and show again that the learned weights reflect domain structure in a sensible way. In the third set (§4.3), we evaluate Meta-PWTD and -PWR in two benchmark RL domains, *bsuite* (Osband et al., 2019) and Atari, and show that our methods do not hinder policy learning in environments not specifically designed to pose idealized long-term credit assignment challenges.

### 4.1. Learned Pairwise Weights in A Simple MDP

Consider the environment represented as a DAG in Figure 2 (left). In each state in the left part of the DAG (states 0–14, the *first phase*), the agent chooses one of two actions but receives no reward. In the remaining states (states 15–44, the *second phase*) the agent has only one action available and it receives a reward of +1 or −1 at each transition. Crucially, the rewards the agent obtains in the second phase are a consequence of the action choices in the first phase because they determine which states are encountered in the



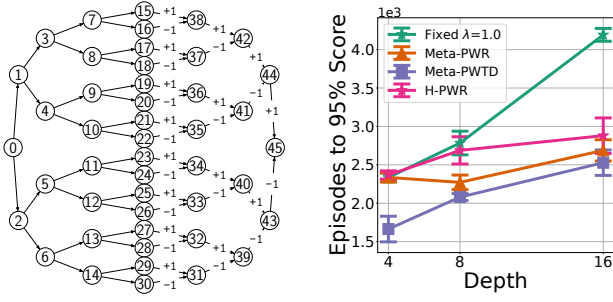


Figure 2. Inner loop-reset and weight visualization experiment: **(Left)** Depth 8 DAG environment with choice of two actions at each state and rewards along transitions. **(Right)** Learning performance of regular return, handcrafted weights, and fixed meta-learned weights. Lower is better.

second phase. There is an interesting credit assignment problem with a nested structure; for example, the action chosen at state 1 determines the reward received later upon transition into state 44. We refer to this environment as the *Depth 8 DAG* and also report results below for depths 4 and 16 with the same nested structure.

For these DAG environments we use a tabular policy, value function, and meta-parameter representations. The parameters  $\theta$ ,  $\psi$ ,  $\phi$ , and  $\eta$  represent the policy, baseline for the weighted return, baseline for the regular return, and meta-parameters respectively. The  $\eta$  parameters are a  $|S| \times |S|$  matrix. The entry on the  $i$ th row and the  $j$ th column defines the pairwise weight for computing the contribution of reward at state  $j$  to the return at state  $i$ . A sigmoid is used to squash the weights to  $[0, 1]$  when computing the updates, and the  $\eta$  parameters are initialized so that the pairwise weights are close to 0.5.

#### Visualizing the Learned Weights via Inner-loop Reset.

One view of Meta-PWTD and -PWR is that they are co-adapting the pairwise weights to the current policy at each point in training. To clearly see the most effective weights that metagradient learned for a random policy, we repeatedly reset the policy parameters to a random initialization while continuing to train the meta-parameters until convergence. More specifically: the meta-parameters  $\eta$  are trained repeatedly by randomly initializing  $\theta$ ,  $\psi$ , and  $\phi$  and running the inner loop for 16 updates for each outer loop update. Following Veeriah et al. (2019) and Zheng et al. (2019), the outer loop objective is evaluated on all 16 trajectories sampled with the updated policies. The gradient of the outer loop objective on the  $i$ th trajectory with respect to  $\eta$  is back-propagated through all of the preceding updates to  $\theta$ . We run the outer loop for 2000 updates. Hyperparameters are provided in the Supplement.

What pairwise weights would accelerate learning in this domain? Figure 3 (top) visualizes a set of *handcrafted* weights

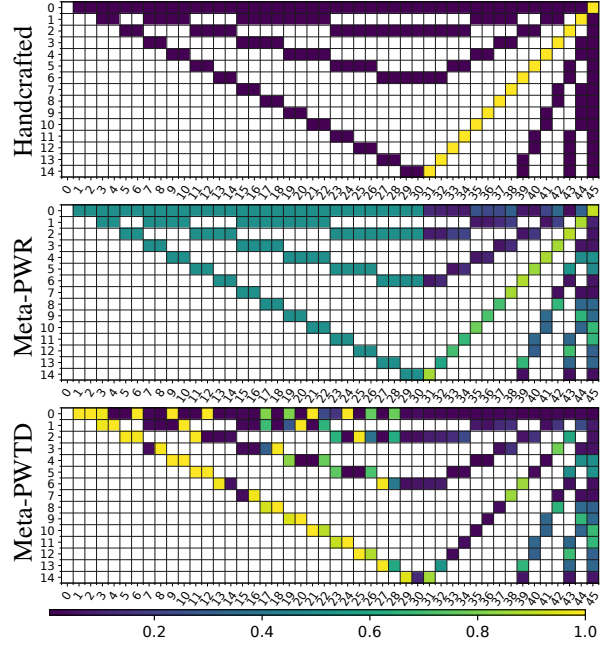


Figure 3. Inner loop-reset weight visualization: **Top:** Handcrafted pairwise weights for Depth 8 DAG; rows and columns correspond to states in Fig. 2. **Middle:** Meta-learned weights for Depth 8 DAG for rewards (Meta-PWR) and **Bottom:** TD-errors (Meta-PWTD).

for  $\hat{\Psi}^{\text{PWR}}$  in the Depth 8 DAG; each row in the grid represents the state in which an action advantage is estimated, and each column the state in which a future reward is experienced. For each state pair  $(s_i, s_j)$  the weight is 1 (yellow) only if the reward at  $s_j$  depends on the action choice at  $s_i$ , else it is zero (dark purple; the white pairs are unreachable). Figure 3 (middle) shows the corresponding weights learned by Meta-PWR via the inner-loop reset procedure. Importantly, the learned pairwise weights have been *increased* for those state pairs in which the handcrafted weights are 1 and have been *decreased* (some to near zero) for those state pairs in which the handcrafted weights are 0; recall they were initialized to 0.5. As in the analysis of the simple domain in §2, these weights will result in lower variance advantage estimates.

The same reset-training procedure was applied to  $\Psi^{\text{PWTD}}$ ; Figure 3 (bottom) visualizes the resulting weights. Since the TD-errors depend on the value function which are nonstationary during agent learning, we expect different weights to emerge at different points in training; the presented weights are but one snapshot. But a clear contrast to reward weighting can be seen: high weights are placed on transitions in the first phase of the DAG, which yield no rewards—because the TD-errors at these transitions do provide signal once the value function begins to be learned. In the Supplement, we explicitly probe the adaptation of  $\Psi^{\text{PWTD}}$  to different points in learning by modifying the value function in reset experi-

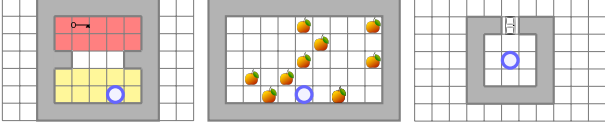


Figure 4. The three Key-to-Door phases. Agent observation is a topdown view of one of the  $7 \times 11$  grids. The blue circle is the agent, the yellow and red areas are possible initial locations for agent and key, respectively.

ments, and show that the weights indeed adapt sensibly to differences in the accuracy of the value function.

**Evaluation of the Learned Pairwise Weights.** After the  $\theta$ -reset training of the pairwise-weights completed, we used them to train a new set of  $\theta$  parameters, fixing the pairwise weights during learning. Figure 2 (right) shows the number of episodes to reach 95% of the maximum score in each DAG, for policies trained with regular returns, handcrafted weights (H-PWR), and meta-learned weights. The meta-learned weights perform as well as and indeed better than the handcrafted weights, and both outperform the regular returns, with the gap increasing for larger DAG-depth. We conjecture that the learned weights performed even better than the handcrafted weights because the learned weights adapted to the dynamics of the inner-loop policy learning procedure and thus could outperform the handcrafted weights, which do not take into account the policy-learning dynamics.

## 4.2. The Key-to-Door Experiments

We evaluated Meta-PWTD and -PWR in a 2D variant of the Key-to-Door (KtD) environment (Hung et al., 2019) that is an elaborate Umbrella problem that was designed to show-off the TVT algorithm’s ability to solve TCA. We varied properties of the domain to vary the credit assignment challenge. We compared the learning performance of our algorithms to a version of  $\hat{\Psi}^{\text{PWR}}$  that uses fixed handcrafted pairwise weights and no metagradient adaptation, as well as to the following **five** baselines (see related work in §1): (a) best fixed- $\lambda$ : Actor-Critic (A2C) (Mnih et al., 2016) with a best fixed  $\lambda$  found via hyperparameter search; (b) TVT (Hung et al., 2019) (using the code accompanying the paper); (c) A2C-RR: a reward redistribution method inspired by RUDDER (Arjona-Medina et al., 2019); (d) Meta- $\lambda(s)$  (Xu et al., 2018): meta-learning a state-dependent function  $\lambda(s)$  for  $\lambda$ -returns; and (e) RGM (Wang et al., 2019): meta-learning a *single* set of weights for generating returns as a linear combination of rewards.

**Environment and Parametric Variation.** KtD is a fixed-horizon episodic task where each episode consists of three 2D gridworld phases (Figure 4, top). In the *Key phase* (15 steps in duration) there is no reward and the agent must

navigate to the key to collect it. The initial locations of the agent and the key are randomly sampled for each episode. In the *Apple phase* (90 steps in duration) the agent collects apples by walking over them; apples disappear once collected. Each apple yields a noisy reward with mean  $\mu$  and variance  $\sigma^2$ . The number of apples is uniformly sampled from  $[1, 20]$  and their locations are randomly sampled. In the *Door phase* (15 steps in duration) the agent starts at the center of a room with a door but can open the door only if it has collected the key earlier. Opening the door yields a reward of 10.

The agent’s observation is a tuple,  $(map, has\_key)$ , where *map* is the top-down view of the current phase rendered in RGB, and *has\_key* is 1 if the agent has collected the key and 0 otherwise. The agent has four navigation actions *up*, *down*, *left*, and *right*. The primary difference between our KtD environment and the original is that our KtD is a top-down view fully-observable environment while the original is a first-person view partially observable environment.

Crucially, picking up the key or not has no bearing on the ability to collect apple rewards. The apples are the noisy rewards that *distract the agent from learning that picking up the key early on leads to a door-reward later*. In our experiments, we evaluate methods on 9 different environments representing combinations of 3 levels of apple reward mean and 3 levels of apple reward variance.

**Neural Network Architecture.** The policy ( $\theta$ ) and the value functions ( $\psi$  and  $\phi$ ) are implemented by separate convolutional neural networks. The *meta-network* ( $\eta$ ) computes the pairwise weight  $w_{ij}$  as follows: First, it embeds the observations  $s_i$  and  $s_j$  and the time difference  $(j - i)$  into separate latent vectors. Then it takes the element-wise product of these three vectors to fuse them into a vector  $h_{ij}$ . Finally it maps  $h_{ij}$  to a scalar output. Sigmoid is applied to the output to bound the weight to  $[0, 1]$ . More details are provided in the Supplement.

**Hyperparameters.** We tuned hyperparameters for each method on the mid-level  $\langle \text{apple mean}, \text{apple variance} \rangle$  configuration  $\langle \mu = 5, \sigma = 25 \rangle$  and kept these parameters fixed for the remaining 8 environments. Each method has a distinct set of parameters (e.g. outer-loop learning rates,  $\lambda$  values) and we used the original papers as guides for the parameter ranges searched over; details are in the Supplement.

**Empirical Results.** Figure 5 presents learning curves for Meta-PWTD, Meta-PWR, and baselines in three KtD configurations (apple reward mean, variance labeled at the top; the remaining configurations are in the Supplement). Learning curves are shown separately for the *total episode return* and the *door phase reward*, the latter a measure of success at the long term credit assignment. Not unexpectedly, H-

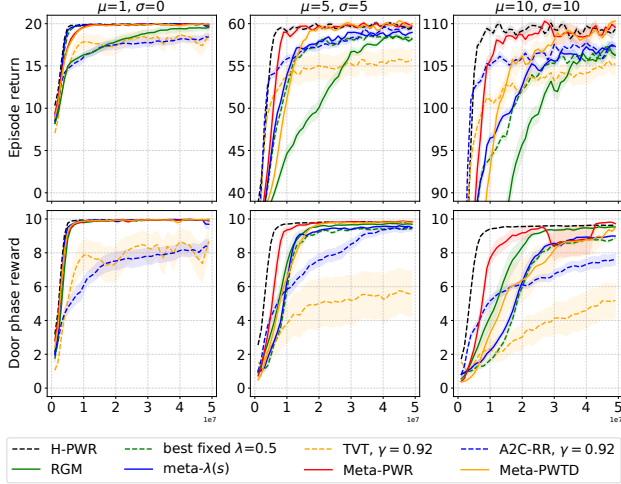


Figure 5. Learning curves for the Key-to-Door domain. Each column corresponds to a different mean ( $\mu$ ) and variance ( $\sigma^2$ ) of apple rewards. The x-axis denotes the number of frames. The y-axis denotes the episode return (in top row) and the door phase reward (in bottom row). The solid curves show the average over 10 independent runs with different random seeds and the shaded area shows the standard errors.

PWR which uses handcrafted pairwise weights performs the best. The gap in performance between H-PWR and the best fixed- $\lambda$  shows that this domain provides a credit assignment challenge that the pairwise-weighted advantage estimate can help with. The TVT and A2C-RR methods used a low discount factor and so relied solely on their heuristics for learning to pick up the key, but neither appears to enable fast learning in this domain. In the door phase, Meta-PWR is generally the fastest learner after H-PWR. Meta-PWTD, though slower, achieves optimal performance. Although RGM performs third best in the door phase, it does not perform well overall, suggesting that the inflexibility of its single set of reward weights (vs. pairwise of Meta-PWR) forces a trade off between short and long-term credit assignment. In summary, Meta-PWR outperforms all the other methods and Meta-PWTD is comparable to the baselines.

Figure 6 presents a visualization of the handcrafted weights for H-PWR (left) and weights learned by Meta-PWR (right). In each heatmap, the element on the  $i$ -th row and the  $j$ -th column denotes  $w_{ij}$ , the pairwise weight for computing the contribution of the reward upon transition to the  $j$ -th state to the return at the  $i$ -th state in the episode. In the heatmap of the handcrafted weights (left), the top-right area has non-zero weights because the rewards in the door phase depend on the actions selected in the key phase. The weights in the remaining part of the top rows are zero because those rewards do not depend on the actions in the key phase. For the same reason, the weights in the middle-right area are

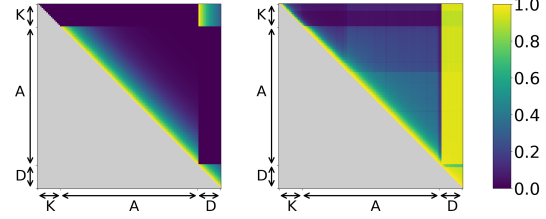


Figure 6. Visualization of pairwise weights in the KtD experiment. **Left:** Handcrafted weights H-PWR. **Right:** The weights learned by Meta-PWR sampled from the  $\mu = 5, \sigma = 5$  setting.

zero as well. The weights in the rest of the area resemble the exponentially discounted weights with a discount factor of 0.92. This steep discounting helps fast learning of collecting apples. The weights learned by metagradients (right) largely resemble the handcrafted weights, which indicate that the metagradient procedure was able to simultaneously learn (1) the important rewards for the key phase are in the door phase, and (2) a quick-discounting set of weights within the apple phase that allows faster learning of collecting apples.

To test the robustness of Meta-PWTD and -PWR to stochastic transitions, we ran a KtD environment where at each time step the action being executed is replaced by a random action with probability 0.1. The learning curves are provided in the Supplement. The results show that Meta-PWTD and -PWR are robust to this kind of stochasticity.

### 4.3. Experiments on Standard RL Benchmarks

Both the DAG and KtD domains are idealized credit assignment problems. It is possible that, in domains outside this idealized class, Meta-PWTD and -PWR are slower to learn than baseline methods because they need time to learn useful weights. To evaluate this possibility we compared them to baseline methods on *bsuite* (Osband et al., 2019) and Atari, both standard benchmarks for RL agents. For these experiments, we did not compare to Meta- $\lambda(s)$  because it performed similarly to the fixed- $\lambda$  baseline in previous experiments as noted in the original paper (Xu et al., 2018).

*bsuite* is a set of unit-tests for RL agents: each domain tests one or more specific RL-challenges, such as exploration, memory, and credit assignment, and each contains several versions varying in difficulty. We selected all domains in *bsuite* that are tagged by “credit assignment”, but with the exception of *Discount Chain*, these domains involve multiple challenges and were not designed solely as idealized credit assignment problems. We ran all methods for 100K episodes in each domain except *Cartpole*, which we ran for 50K episodes. Each run was repeated 3 times with different random seeds. The resulting regret scores are summarized in Table 1. For *Discount Chain* Meta-PWR improved regret by a large amount. More generally, Meta-

Table 1. Total regrets on selected `bsuite` domains (lower is better).

	Catch	Catch Noise	Catch Scale	Umbr. Length	Umbr. Distract	Cartpole	Discount Chain
A2C	5975	42221	56800	38050	37524	76874	3554
A2C-RR	<b>5950</b>	42295	57033	38083	37433	71506	3548
RGM	7849	48268	54421	40397	40159	119102	2444
Meta-PWTD	6096	<b>41106</b>	<b>48199</b>	<b>37973</b>	37226	65945	1040
Meta-PWR	5967	43076	49361	38168	<b>36554</b>	<b>61752</b>	<b>161</b>

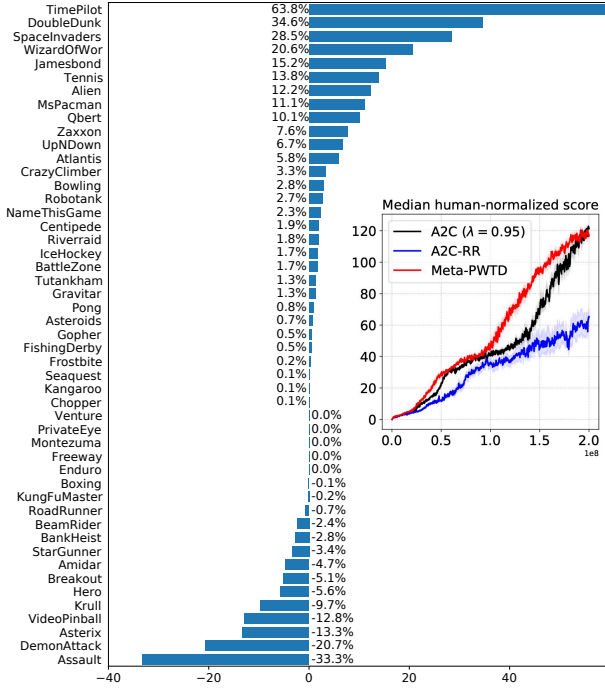


Figure 7. Relative performance of Meta-PWTD over A2C ( $\lambda = 0.95$ ). All scores are averaged over 5 independent runs with different random seeds. **Inset:** Learning curves of median human normalized score of all 49 Atari games. Shaded area shows the standard error over 5 runs.

PWTD or -PWR achieved the lowest total regrets in all domains except for *Catch*, in which A2C-RR achieved the lowest. It shows that Meta-PWTD and Meta-PWR perform better than or comparably to the baseline methods even in domains without the idealized long-term TCA structure present in Umbrella-like problems such as Key-to-Door.

To test scalability to high-dimensional environments, we conducted experiments on Atari. Atari games often have long episodes of  $> 1000$  steps thus episode truncation is required. Meta-PWTD and -PWR can deal with truncated episodes by using the value function at the state of truncation to correct for the missing rest of the episode. Using a value function to handle truncation in PWR would be analogous to using an  $n$ -step estimator while using the value function to handle truncation in PWTD is analogous to using

a truncated  $\lambda$ -estimator. Since truncated PWTD is smoother than truncated PWR (early experiments confirmed this intuition) and needs nearly zero modification, we focused on the former. Note that truncated-PWTD can precisely implement the truncated  $\lambda$ -return by setting the weight to  $(\gamma\lambda)^{(t'-t-1)}$  for the correction value function at the state of truncation. TVT and RGM are precluded because they require complete episodes to apply updates. Therefore, we only ran Meta-PWTD, A2C-RR and A2C. For each we conducted hyperparameter search on a subset of 6 games (Asterix, BeamRider, Breakout, Qbert, Seaquest, and SpaceInvaders), and ran each method on 49 games with the fixed set of hyperparameters; see Supplement for details. An important hyperparameter for the A2C baseline is  $\lambda$ , which was set to 0.95. Following convention, we ran each method for 200 million frames on each game.

Figure 7 (inset) shows the median human-normalized score during training. Meta-PWCA performed slightly better than A2C over the entire period, and both performed better than A2C-RR<sup>1</sup>. Figure 7 shows the relative performance of Meta-PWTD over A2C. Meta-PWTD outperforms A2C in 30 games, underperforms in 14, and ties in 5. These results show that Meta-PWTD can scale to high-dimensional environments like Atari. We conjecture that Meta-PWTD provides a benefit in games with embedded Umbrella problems but this is hard to verify directly.

## 5. Conclusion

We presented two new advantage estimators with pairwise weight functions as parameters to be used in policy gradient algorithms, and a metagradient algorithm for learning the pairwise weight functions. Simple analysis and empirical work confirmed that the additional flexibility in our advantage estimators can be useful in domains with delayed consequences of actions, e.g., in Umbrella-like problems. Empirical work also confirmed that the metagradient algorithm can learn the pairwise weights fast enough to be useful for policy learning, even in large-scale environments like Atari.

<sup>1</sup>The paper introducing RUDDER incorporated many ideas in addition to reward redistribution into PPO (Schulman et al., 2017) and was able to outperform PPO but that code is not available.



## Acknowledgement

This work was supported by DARPA’s L2M program as well as a grant from the Open Philanthropy Project to the Center for Human Compatible AI. Any opinions, findings, conclusions, or recommendations expressed here are those of the authors and do not necessarily reflect the views of the sponsors.

## References

- Arjona-Medina, J. A., Gillhofer, M., Widrich, M., Unterthiner, T., Brandstetter, J., and Hochreiter, S. Rudder: Return decomposition for delayed rewards. In *Advances in Neural Information Processing Systems*, pp. 13544–13555, 2019.
- Dhariwal, P., Hesse, C., Klimov, O., Nichol, A., Plappert, M., Radford, A., Schulman, J., Sidor, S., Wu, Y., and Zhokhov, P. Openai baselines. <https://github.com/openai/baselines>, 2017.
- Harutyunyan, A., Dabney, W., Mesnard, T., Azar, M. G., Piot, B., Heess, N., van Hasselt, H. P., Wayne, G., Singh, S., Precup, D., et al. Hindsight credit assignment. In *Advances in neural information processing systems*, pp. 12467–12476, 2019.
- Hochreiter, S. and Schmidhuber, J. Long short-term memory. *Neural computation*, 9(8):1735–1780, 1997.
- Hung, C.-C., Lillicrap, T., Abramson, J., Wu, Y., Mirza, M., Carnevale, F., Ahuja, A., and Wayne, G. Optimizing agent behavior over long time scales by transporting value. *Nature communications*, 10(1):1–12, 2019.
- Kingma, D. P. and Ba, J. Adam: A method for stochastic optimization. *arXiv preprint arXiv:1412.6980*, 2014.
- Mnih, V., Kavukcuoglu, K., Silver, D., Rusu, A. A., Veness, J., Bellemare, M. G., Graves, A., Riedmiller, M., Fidjeland, A. K., Ostrovski, G., et al. Human-level control through deep reinforcement learning. *nature*, 518(7540): 529–533, 2015.
- Mnih, V., Badia, A. P., Mirza, M., Graves, A., Lillicrap, T., Harley, T., Silver, D., and Kavukcuoglu, K. Asynchronous methods for deep reinforcement learning. In *International conference on machine learning*, pp. 1928–1937, 2016.
- Oh, J., Hessel, M., Czarnecki, W. M., Xu, Z., van Hasselt, H. P., Singh, S., and Silver, D. Discovering reinforcement learning algorithms. *Advances in Neural Information Processing Systems*, 33, 2020.
- Osband, I., Doron, Y., Hessel, M., Aslanides, J., Sezener, E., Saraiva, A., McKinney, K., Lattimore, T., Szepevari, C., Singh, S., et al. Behaviour suite for reinforcement learning. *arXiv preprint arXiv:1908.03568*, 2019.
- Perez, E., Strub, F., De Vries, H., Dumoulin, V., and Courville, A. Film: Visual reasoning with a general conditioning layer. In *Thirty-Second AAAI Conference on Artificial Intelligence*, 2018.
- Rajendran, J., Lewis, R., Veeriah, V., Lee, H., and Singh, S. How should an agent practice? *arXiv preprint arXiv:1912.07045*, 2019.
- Schulman, J., Moritz, P., Levine, S., Jordan, M., and Abbeel, P. High-dimensional continuous control using generalized advantage estimation. *arXiv preprint arXiv:1506.02438*, 2015.
- Schulman, J., Wolski, F., Dhariwal, P., Radford, A., and Klimov, O. Proximal policy optimization algorithms. *arXiv preprint arXiv:1707.06347*, 2017.
- Sutton, R. S. Learning to predict by the methods of temporal differences. *Machine learning*, 3(1):9–44, 1988.
- Sutton, R. S., McAllester, D. A., Singh, S. P., and Mansour, Y. Policy gradient methods for reinforcement learning with function approximation. In *Advances in neural information processing systems*, pp. 1057–1063, 2000.
- Vaswani, A., Shazeer, N., Parmar, N., Uszkoreit, J., Jones, L., Gomez, A. N., Kaiser, Ł., and Polosukhin, I. Attention is all you need. In *Advances in neural information processing systems*, pp. 5998–6008, 2017.
- Veeriah, V., Hessel, M., Xu, Z., Rajendran, J., Lewis, R. L., Oh, J., van Hasselt, H. P., Silver, D., and Singh, S. Discovery of useful questions as auxiliary tasks. In *Advances in Neural Information Processing Systems*, pp. 9306–9317, 2019.
- Wang, Y., Ye, Q., and Liu, T.-Y. Beyond exponentially discounted sum: Automatic learning of return function. *arXiv preprint arXiv:1905.11591*, 2019.
- Williams, R. J. Simple statistical gradient-following algorithms for connectionist reinforcement learning. *Machine learning*, 8(3-4):229–256, 1992.
- Xu, Z., van Hasselt, H. P., and Silver, D. Meta-gradient reinforcement learning. In *Advances in neural information processing systems*, pp. 2396–2407, 2018.
- Xu, Z., van Hasselt, H., Hessel, M., Oh, J., Singh, S., and Silver, D. Meta-gradient reinforcement learning with an objective discovered online. *arXiv preprint arXiv:2007.08433*, 2020.

Zahavy, T., Xu, Z., Veeriah, V., Hessel, M., Oh, J., van Hasselt, H. P., Silver, D., and Singh, S. A self-tuning actor-critic algorithm. *Advances in Neural Information Processing Systems*, 33, 2020.

Zheng, Z., Oh, J., and Singh, S. On learning intrinsic rewards for policy gradient methods. In *Advances in Neural Information Processing Systems*, pp. 4644–4654, 2018.

Zheng, Z., Oh, J., Hessel, M., Xu, Z., Kroiss, M., van Hasselt, H., Silver, D., and Singh, S. What can learned intrinsic rewards capture? *arXiv preprint arXiv:1912.05500*, 2019.

## A. DAG Experiments

Three algorithms were compared in a tabular domain. In this appendix, the hyperparameter configurations of the three algorithms are provided in Section A.1 and more detailed results are reported in Section A.3.

### A.1. Hyperparameters

An informal hyperparameter search was conducted for the three algorithms. Fixed- $\lambda$  uses the Adam optimizer (Kingma & Ba, 2014) with learning rate 0.01,  $\beta_1 = 0$ ,  $\beta_2 = 0.999$ , and  $\epsilon = 10^{-8}$ . Updates are computed on batches consisting of 8 full episodes. We found  $\lambda = 1$  the best, better than any smaller values. We used a discount factor  $\gamma = 1$  and an entropy regularization coefficient 0.001. The inner loop of Meta-PWTD, Meta-PWR, and H-PWR share hyperparameters with the fixed- $\lambda$  baseline, except that  $\lambda$  is not used. For Meta-PWTD and Meta-PWR, the outer-loop optimizer is Adam with the same hyperparameters as the inner-loop optimizer. Outer-loop gradient is clipped to 0.5 by global norm. The weight matrix  $\eta$  is initialized from uniform distribution in range  $[-0.01, 0.01]$ .

### A.2. Learning TD-error weights weights with different value functions.

In the main paper we show that the weights learned for rewards converge to a fixed weight matrix, which resembles the handcrafted weights we believe are useful for variance reduction (see Figure 10, Figure 11, and Figure 12 for visualizations of the weights). While the reward weighting may change somewhat during training, there exists fixed sets of weights that are beneficial throughout the training. During the training of an actor-critic algorithm, the TD-errors change as the value function fits to the current policy. While we have demonstrated that we can learn fixed weights for the TD-errors that speed up learning considerably, in more complicated domains a fixed weighting scheme may end up hurting the performance. To shed light into weight learning in a setting where the value function is changing, we consider the DAG reset-training setting but instead of learning the value function with the policy, we use the optimal value function, which we mask to simulate non-stationary learning. By masking we mean setting the value to zero for all states up to certain depth in the DAG environment, making the optimal value function less informative.

In Figure 8, three cases of value masking are shown in the depth 8 DAG environment where the optimal value function has been masked to depth 0, 4, and 8. In the mask depth 0 case, the weights for the TD-errors have mostly changed in the parts of the weight matrix before column 30. Column 30 corresponds to the last state of the middle-layer of the DAG that splits the states where the agent can act from the states where the agent receives rewards. When values are masked up to depth 4, the TD-error weighting shifts. State 14 is the last state at depth 4, so all weights before that are unchanged from the initialization. Note that at mask depths 0 and 4, no weights are placed on the states in the weight matrix after column 30. Finally, at depth 8, all of the value function has been masked out and the TD-error weighting has converged to visually similar weights as the reward weights, which is expected as the TD-errors computed with the fully masked value function consist only of the rewards. The learned weights in Figure 8 show that Meta-PWTD will learn different kinds of weightings depending on the value function.

### A.3. Additional Empirical Results

Learning curves in the DAG environment are presented in Figure 9. Handcrafted and learned weights in the 4, 8, and 16 deep DAG environment variants are presented in Figures 10, 11, and 12.

## B. Key-to-Door Experiments

### B.1. Environment Description

Key-to-Door (KtD) is a fixed-horizon episodic task where each episode consists of three 2D gridworld phases.

In the *Key phase* (duration 15 steps), there is no reward and the agent must navigate in a  $5 \times 5$  map to collect a key. The key disappears once collected. The initial locations of the agent and the key are randomly sampled in each episode.

In the *Apple phase* (duration 90 steps), the agent collects apples in a  $5 \times 9$  map by walking over them; apples disappear once collected. Each apple yields a noisy reward with mean  $\mu$  and variance  $\sigma^2$ . Specifically, each apple yields a reward of  $r = \frac{\sigma^2}{\mu^2} + 1$  with probability  $\frac{1}{r}$  or a reward of 0 with probability  $1 - \frac{1}{r}$ . This sampling procedure is consistent with the original TVT paper (Hung et al., 2019). The number of apples is uniformly sampled from  $[1, 20]$  and their locations are

randomly sampled.

In the *Door phase* (duration 15 steps), the agent starts at the center of a  $3 \times 3$  room with a door. The agent can open the door only if it has collected the key in the earlier Key phase. The door disappears after being opened. Successfully opening the door yields a reward of 10.

The agent’s observation is a tuple,  $(map, has\_key)$ . *map* is the top-down view of the current phase and is rendered in an RGB representation. *has\\_key* is a binary channel which is 1 if the agent has already collected the key and 0 otherwise. The agent has 4 actions which correspond to moving *up*, *down*, *left*, and *right*. The primary difference between our KtD environment and the original is that our environment is fully observable; the original is partially observable. This difference is reflected in two modifications: the agent observes the top-down view of the map rather than the first-person view, and the agent observes whether it has collected the key.

For the stochastic dynamics variant, the action being executed is replaced by a random action with probability 0.1 for each time step.

## B.2. Implementation Details

All methods use A2C (Mnih et al., 2016) as the policy optimization algorithm. 16 actors are used to generate data. The rollout length is equal to the episode length, 120 in this case. For each method described below, we conducted a hyperparameter search in the  $\mu = 5$  and  $\sigma = 5$  KtD environment and selected the best-performing hyperparameters. Then the hyperparameters were fixed for all the other 8 environment configurations. Each candidate hyperparameter combination was run with three different random seeds for 50 million frames. The best hyperparameter combination was determined to be the one that first achieved 57 in episode return, i.e., 95% of the maximum possible. The following hyperparameter settings are shared across all methods unless otherwise noted: learning rate  $2 * 10^{-4}$ , and Adam  $\beta_1 = 0$ , Adam  $\beta_2 = 0.999$ , Adam  $\epsilon = 10^{-8}$ , discount factor  $\gamma = 0.998$ , and entropy regularization coefficient 0.05. The advantage estimates are standardized in a batch of trajectories before computing the policy gradient loss (Dhariwal et al., 2017) unless otherwise noted.

**A Standard Perception module.** A standard perception module is used by all method to process the observation  $s$  to a latent vector  $h$ . The observation  $s$  is a tuple,  $(map, has\_key)$ . *map* is the top-down view of the current phase that has shape  $(7, 11, 3)$ , where the last dimension is the RGB channels. *has\\_key* is a binary channel which is 1 if the agent has already collected the key and 0 otherwise. *map* is processed by two convolutional layers with 16 and 32 filters respectively. Both convolutional layers use  $3 \times 3$  kernels and are followed by ReLU activation. The output of the last convolutional layer is then flattened and processed by Dense(512) - ReLU. The binary input *has\\_key* is concatenated with the ReLU layer output. Finally, the concatenated vector is further processed by a MLP: Dense(512) - ReLU - Dense(256) - ReLU. We denote the final output of the perception module as  $h$ .

**Fixed- $\lambda$**  The fixed- $\lambda$  baseline implements the standard A2C algorithm. The policy and value function are implemented by two separate neural networks consisting of a perception module and an output layer without any parameter sharing. The policy network maps  $h$  to the policy logits via a single dense layer. The value network maps  $h$  to a single scalar via a single dense layer. We label this baseline fixed- $\lambda$  to underline the importance of the eligibility trace parameter  $\lambda$ . We searched for all combinations of the following hyperparameter sets:  $\lambda$  in  $\{1.0, 0.99, 0.98, 0.95, 0.9, 0.8, 0.5, 0\}$ , and learning rate in  $\{10^{-3}, 2 * 10^{-4}, 5 * 10^{-5}, 10^{-5}\}$ . The best performing set of hyperparameters is  $\lambda = 0.5$  and learning rate  $2 * 10^{-4}$ .

**Meta-PWTD** The policy ( $\theta$ ) and value function for the original return ( $\psi$ ) have the same network architecture as in the fixed- $\lambda$  baseline. The value function for the weighted sum of rewards ( $\phi$ ) has identical architecture as the value function for the original return ( $\psi$ ). The meta-network ( $\eta$ ) computes the weights as follows. For each episode, the inputs to the meta-network is a sequence  $(s_0, \delta_1, s_1, \dots, \delta_T, s_T)$ . Note that the TD-error  $\delta_i$  is part of the inputs. The meta-network first maps each  $s_t$  ( $0 \leq t \leq T$ ) into a latent vector  $h_t$  with a standard perception module. The meta-network ( $\eta$ ) shares the perception module with the value function for the original return ( $\psi$ ). No gradient is back-propagated from the meta-network to the shared perception module. A dense layer with 256 hidden units maps  $h_i$  ( $0 \leq i < T$ ) into  $h_i^{row}$ ; a separate dense layer with 256 units maps  $h_j \oplus \delta_j$  ( $0 < j \leq T$ ) into  $h_j^{col}$  where  $\oplus$  denotes concatenation. The TD-error  $\delta_j$  is clipped to  $[-1, 1]$  before concatenation. Both dense layers are followed by ReLU activation. Another dense layer with 256 units maps the time interval  $(j - i)$  ( $0 \leq i < j \leq T$ ) to a latent vector  $td_{ij}$ .  $h_i^{row}$ ,  $h_j^{col}$ , and  $td_{ij}$  are element-wise multiplied to fuse the three latent vectors into one vector  $h_{ij}$ :  $h_{ij} = (h_i^{row} + 1) * (h_j^{col} + 1) * (td_{ij} + 1)$ . Note that every vector is shifted by a constant 1 before the multiplication to mitigate gradient vanishing at the beginning of training (Perez et al., 2018). The



latent vectors  $h_{ij}$  ( $0 \leq i < j \leq T$ ) are normalized by

$$h'_{ijd} = \gamma_d \frac{(h_{ijd} - \mu_d)}{\sigma_d} + \beta_d \quad (1 \leq d \leq 256),$$

where

$$\mu_d = \frac{2}{T * (T + 1)} \sum_{0 \leq i < j \leq T} h_{ijd}$$

and

$$\sigma_d = \sqrt{\frac{2}{T * (T + 1)} \sum_{0 \leq i < j \leq T} (h_{ijd} - \mu_d)^2}$$

are the empirical mean and standard deviation of  $h_{ij}$  respectively.  $\gamma_d$  and  $\beta_d$  are trainable parameters. ReLU activation is applied to  $h'_{ij}$ . Finally, the output layer maps each  $h'_{ij}$  into  $w_{ij}$ . The initial weights for the output layer is scaled by a factor 0.01 so that the initial outputs are closer to uniform. We applied Sigmoid activation on the outputs to bound the weights to  $(0, 1)$ . As for hyperparameters, the entropy regularization coefficient is set to 0.05. For the inner loop, we used the Adam optimizer with learning rate  $2 * 10^{-4}$ ,  $\beta_1 = 0$ ,  $\beta_2 = 0.999$ , and  $\epsilon = 10^{-8}$ . For the outer loop, we used the Adam optimizer with learning rate  $2 * 10^{-5}$ ,  $\beta_1 = 0$ ,  $\beta_2 = 0.999$ , and  $\epsilon = 10^{-8}$ .

**Meta-PWR** Meta-PWR uses the same neural network architecture as Meta-PWTD. The only difference is that Meta-PWR does *not* take the reward  $r_i$  or the TD-error  $\delta_i$  as inputs. The hyperparameters for Meta-PWR are also the same as those for Meta-PWTD.

**H-PWR** The policy and value function for the weighted sum of rewards have the same network architecture as in the fixed- $\lambda$  baseline. We handcraft pairwise weights for the KtD domain to take advantage of the known credit assignment structure that can be described as follows: The policy learning in the key phase depends only on the reward in the door phase, the policy learning in the apple phase does not depend on the other phases, and while the picking up the key or not impacts the reward in the door phase, the reward in the door phase is still instantaneous. The weights are set so that in the key phase, the rewards in the apple phase receive a zero weight and the rewards in the door phase are discounted starting from the first timestep of the door phase. Weights that compute discounting equivalent to  $\gamma = 0.92$  are applied in the apple phase and door phase. An illustration of the learned weights is presented in Figure 3 in the main paper. H-PWR uses the same hyperparameters as fixed- $\lambda$  except  $\gamma$ , which does not apply and  $\lambda$ , which is set to 1.0. No hyperparameter search is conducted specifically for H-PWR.

**Meta- $\lambda(s)$**  The policy ( $\theta$ ) and value function for the original return ( $\psi$ ) have the same network architecture as in the fixed- $\lambda$  baseline. The value function for the weighted sum of rewards ( $\phi$ ) has identical architecture as the value function for the original return ( $\psi$ ). The meta-network ( $\eta$ ) maps a state  $s_t$  to a scalar  $\lambda(s_t) \in (0, 1)$ . The meta-network first maps the observation  $s_t$  to a latent vector  $h_t$  with the standard perception module and then maps  $h_t$  to a single scalar  $\lambda(s_t)$  via a single dense layer. Sigmoid is applied to the output of the meta-network to bound it to  $(0, 1)$ . We searched for the outer-loop learning rate in  $\{10^{-4}, 2 * 10^{-5}, 5 * 10^{-6}, 10^{-6}\}$ . The best performing outer-loop learning rate is  $10^{-6}$ . The outer-loop  $\lambda$  is set to 1.0 without search.

**RGM** The policy ( $\theta$ ) and value function for the original return ( $\psi$ ) have the same network architecture as in the fixed- $\lambda$  baseline. The value function for the weighted sum of rewards ( $\phi$ ) has identical architecture as the value function for the original return ( $\psi$ ). For an episode  $\tau = (s_0, a_0, r_1, s_1, \dots, s_T)$ , the meta-network first maps each  $s_t$  ( $0 \leq t \leq T$ ) to  $h_t^0$  by a shared standard perception module. Then it concatenates  $h_t^0$  with  $r_t$  and the one-hot representation of  $a_t$ . Four Transformer blocks (Vaswani et al., 2017) are applied on the concatenated features, each block with four attention heads. We denote the output of the final Transformer block as  $h_t^4$  ( $0 \leq t \leq T$ ). Finally, a shared linear layer maps each  $h_t^4$  to  $\beta_t$ , the weight on the reward  $r_t$ . We searched for the outer-loop learning rate in  $\{10^{-4}, 10^{-5}, 10^{-6}, 10^{-7}\}$ , as suggested by the original paper (Wang et al., 2019). The best performing outer-loop learning rate is  $10^{-6}$ . The outer-loop  $\lambda$  is set to 1.0 without search.

**TVT** We adopted the agent architecture from the open-source implementation accompanying the original TVT paper (<https://github.com/deepmind/deepmind-research/tree/master/tvt>). The only difference is that we replaced the convolutional

neural network torso in the original code with the standard perception module. We searched for all combinations of the following hyperparameter sets: the read strength threshold for triggering the splice event in  $\{1, 2\}$  and the learning rate in  $\{10^{-3}, 2 * 10^{-4}, 5 * 10^{-5}, 10^{-5}\}$ . The best performing set of hyperparameters are 1 for the read strength threshold and  $2 * 10^{-4}$  for the learning rate. We did not use advantage standardization for TVT because we found that it hurt the performance in the KtD domain. We used the Adam optimizer parameters  $\beta_1 = 0$ ,  $\beta_2 = 0.95$ , and  $\epsilon = 10^{-6}$ , as the open-source implementation suggested. We also set  $\lambda = 0.92$  and  $\gamma = 0.92$  following the original implementation.

**A2C-RR** We pick the main ideas from RUDDER (Arjona-Medina et al., 2019) and implement them in an algorithm we call A2C-RR. RUDDER uses contribution analysis to redistribute rewards in a RL episode. The high-level idea is that since the environment rewards may be delayed from the transitions that resulted in them, contribution analysis may be used to compute how much of the total return is explained by any particular transition. In effect, this drives the expected future return to zero because any reward that can be expected at any given timestep will be included in the redistributed reward, eliminating the delay and leading to faster learning of the RL agent. The method is based on learning a LSTM-network, which predicts the total episodic return at every timestep. The redistributed reward is computed as the difference of return predictions on consecutive timesteps.

Compared to the full RUDDER algorithm, A2C-RR incorporates a few changes to isolate some of the core ideas of the reward redistribution module and make the algorithm more directly comparable to the other A2C-based algorithms discussed in this paper. We use the LSTM cell-architecture proposed in the RUDDER paper and train it from samples stored in a replay buffer. In the KtD-experiments, we do not use the “quality” weighted advantage estimate proposed in the paper due to the random noise in the episodic return, which we deem too high variance for reliable estimation of the redistribution quality. Instead we mix the original and redistribution-based advantages at a fixed ratio. We recognize that omitting some of the features of the full RUDDER algorithm may adversely impact the reward redistribution and therefore the agent learning performance. Nevertheless, we believe the reward redistribution idea is an interesting take on a similar idea as the pairwise weighting studied in this paper and therefore provide our implementation – A2C-RR – of that idea as a baseline.

The regular frames and delta frames (as described in the paper) are processed by the standard perception module. The perception module outputs and the one-hot encoded action are concatenated and processed by Dense(512) - ReLU. The output of the ReLU layer is the input for the reward redistribution model. As suggested in the paper, the reward redistribution model is a LSTM without a forget gate and output gate. The cell input only receives forward connections and the gates only receive recurrent connections. All of the layers in the LSTM have 64 units. We chose not to use the prioritized replay buffer described in the paper due to the high variance of the returns in the KtD environment. For the same reason we did not use the quality measure, which is also described in the paper, for mixing the RUDDER advantage and regular advantage. Instead, we used a fixed mixing coefficient, which we searched for. The advantage is standardized after the mixing. We implemented an auxiliary task described in the paper, where the total return prediction loss is applied at every step of the episode. The reward redistribution model is trained for 10 randomly sampled batches of size 8 from a circular buffer holding the past 128 trajectories between each policy update. We set the number of updates to 10 via an informal hyperparameter search in the  $\mu = 5$ ,  $\sigma = 5$  KtD setting, where we found that training 10 times between each update performs better than 5 but further increasing it did not yield further large improvements. The reward redistribution model is trained with Adam with learning rate  $10^{-4}$ ,  $\beta_1 = 0.9$ , and  $\beta_2 = 0.999$ . We applied a L2 weight regularizer with coefficient  $10^{-7}$ . We searched for all combinations of the following hyperparameter sets:  $\gamma$  in  $(0.92, 1.0)$ ,  $\lambda$  in  $(1.0, 0.95, 0.5)$ , auxiliary task coefficient in  $(0.0, 0.5)$ , and advantage mixing coefficient in  $(0.5, 1.0)$ . The best performing set of hyperparameters is  $\gamma = 0.92$ ,  $\lambda = 0.5$ , auxiliary task coefficient 0.0, and advantage mixing coefficient 0.5.

### B.3. Additional Empirical Results

We ran all of the methods described above in 9 variants of the KtD environment. Figure 13, Figure 14, and Figure 15 shows the episode return, the total reward in the door phase, and the total reward in the apple phase respectively.

Noticing that the KtD domain has deterministic dynamics, we also conducted experiments on a stochastic KtD domain where the action being executed is replaced by a random action with probability 0.1 for each time step. The corresponding results are presented in Figure 16, Figure 17, and Figure 18. In general, Meta-PWTD and Meta-PWR still perform better than the baseline methods regardless of the stochasticity in the transition dynamics.

## C. bsuite Experiments

### C.1. Environment Description

We selected 7 tasks which were associated with the “credit assignment” tag from `bsuite`. They present a variety of credit assignment structures, including the umbrella problem in §3 in the main text. Additionally, all domains except *Discount Chain* have multiple tags which create additional challenges than temporal credit assignment. We ran all different variants of every task, each with 3 different random seeds. Unlike the standard data regime of `bsuite`, we ran each task for 100K episodes for all methods to calculate the total regret score, except *Cartpole*, which we ran for 50K episodes. We refer the readers to the original `bsuite` paper (Osband et al., 2019) and the accompanying github repository (<https://github.com/deepmind/bsuite>) for further details.

### C.2. Implementation Details

Most methods use a similar neural network architecture as described in §B.2. There are two common differences. First, we used 1 single actor instead of 16 parallel actors for generating data. Second, the standard perception module is replaced by a 2-layer MLP with 64 hidden units and ReLU activation each layer, because the inputs are vectors instead of images in `bsuite`. Further architecture differences and hyperparameters are described below.

**Actor-critic baseline.** The entropy regularization weight is set to 0.05. we used the Adam optimizer with learning rate  $3 * 10^{-4}$ ,  $\beta_1 = 0$ ,  $\beta_2 = 0.999$ , and  $\epsilon = 10^{-8}$ .

**Meta-PWTD and Meta-PWR** Besides the perception module, there are two more differences with §B.2. First, the meta-network ( $\eta$ ) and the value function for the original return ( $\psi$ ) use separate perception module instead of sharing. Second, all the hidden layers after the perception module use 64 hidden units instead of 256. The entropy regularization weight is set to 0.05. For the inner loop, we used the Adam optimizer with learning rate  $3 * 10^{-4}$ ,  $\beta_1 = 0$ ,  $\beta_2 = 0.999$ , and  $\epsilon = 10^{-8}$ . For the outer loop, we used the Adam optimizer with learning rate  $3 * 10^{-5}$ ,  $\beta_1 = 0$ ,  $\beta_2 = 0.999$ , and  $\epsilon = 10^{-8}$ . Outer-loop gradient is clipped to 0.01 by global norm.

**RGM** The entropy regularization weight is set to 0.05. For the inner loop, we used the Adam optimizer with learning rate  $3 * 10^{-4}$ ,  $\beta_1 = 0$ ,  $\beta_2 = 0.999$ , and  $\epsilon = 10^{-8}$ . For the outer loop, we used the Adam optimizer with learning rate  $1 * 10^{-4}$ ,  $\beta_1 = 0$ ,  $\beta_2 = 0.999$ , and  $\epsilon = 10^{-8}$ .

**A2C-RR** Apart from the perception module, the same A2C-RR implementation was used for `bsuite` as was used for KtD experiments. The actor-critic was trained with the same hyperparameters as the Actor-Critic baseline for `bsuite`. The LSTM was trained with the same hyperparameters as in KtD.

## D. Atari Experiment

### D.1. Implementation Details

Most methods use a similar neural network architecture as described in §B.2. There are two common differences. First, we generate 20-step trajectories instead of full episodes for each policy update, following the original A2C implementation (Mnih et al., 2016). Second, the standard perception module is replaced by the convolutional neural network architecture used in (Mnih et al., 2015). Further architecture differences and hyperparameters are described below.

**A2C** The policy and the value function share the perception module. The value loss coefficient is 0.5. The entropy regularization coefficient is 0.01. We used the RMSProp optimizer with learning rate 0.0007, decay 0.99, and  $\epsilon = 10^{-5}$ . The gradient is clipped to 0.5 by global norm. The discount factor  $\gamma$  is 0.99. We searched for the eligibility traces parameter  $\lambda$  in  $\{0.8, 0.9, 0.95, 0.98, 0.99, 1\}$  and selected 0.95.

**Meta-PWTD** The inner-loop hyperparameters are exactly the same as the A2C baseline. For the outer loop, We applied an entropy regularization as well to stabilize training. The coefficient is 0.01. The outer loop uses the Adam optimizer with learning rate 0.00003,  $\beta_1 = 0$ ,  $\beta_2 = 0.999$ , and  $\epsilon = 10^{-8}$ . The outer-loop gradient is clipped to 0.05 by global norm.

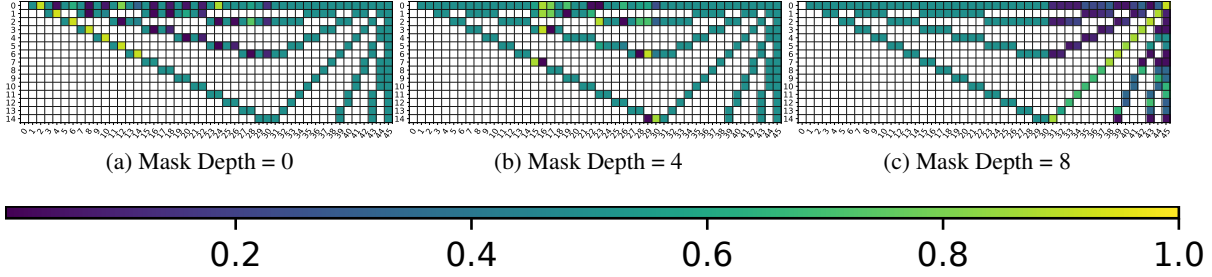


Figure 8. Meta-PWTD inner loop-reset weight visualization experiment with masked optimal value function. Figures (a,b,c) show the learned weight matrices for mask depths 0, 4, and 8 respectively.

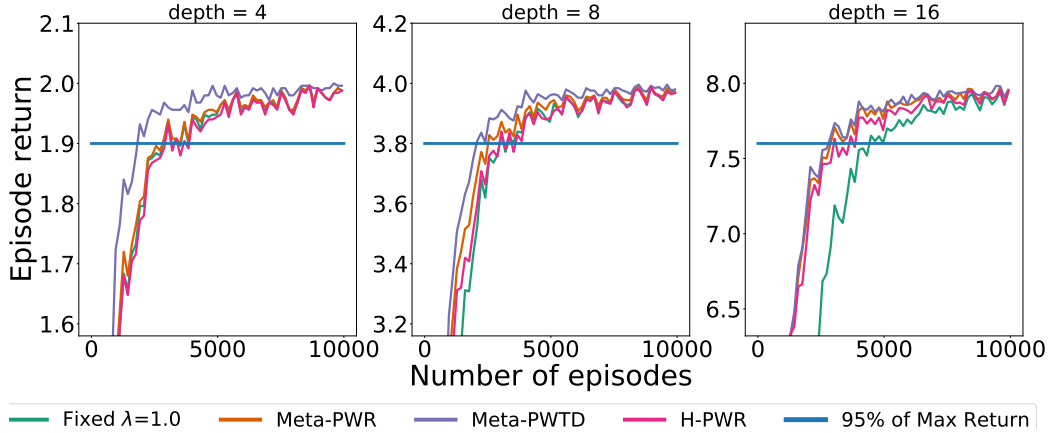


Figure 9. Learning curves in the DAG environments. Each curve is the mean of 5 seeds. The line for 95% of max return is added to help contextualize these learning curves with Figure 2 in the main paper.

**A2C-RR** To handle the variable length episodes in Atari, we chunk the trajectories as described in the RUDDER paper (Arjona-Medina et al., 2019). Unlike RUDDER, A2C-RR uses a circular replay buffer, to which all trajectories are added and samples training batches from the buffer uniformly. We use the quality measure described in the RUDDER paper for mixing the advantage estimates to the A2C-RR implementation for Atari. The quality is computed as described in the paper, and used for mixing the advantage computed with the environment rewards and the one computed with the redistributed rewards. The quality is also used as the coefficient for the mean-squared error loss used for training the baseline for the redistributed reward. The LSTM is trained for a maximum of 100 LSTM epochs every 100 actor-critic training iterations. If the quality of the last 40 LSTM training trajectories is positive after updating the LSTM, the LSTM training is stopped. For training the LSTM, we normalize the rewards by the maximum return encountered so far and multiply the normalized rewards by 10. Before mixing the regular and the redistributed advantages, we denormalize the redistributed rewards by inverting the normalization process above. The inputs to the LSTM are the delta-frames and one-hot encoded actions. In the RUDDER paper, a more sophisticated exploration strategy is used for collecting data. We did not implement it for a fair comparison to other methods.

A2C-RR uses the same A2C agent as the Fixed- $\lambda$  baseline, with the same hyperparameters. Apart from the differences described above, the LSTM training hyperparameters are from the RUDDER paper (Arjona-Medina et al., 2019). The LSTM is trained with trajectories of length 512, further split into chunks of length 128. The LSTM training batch size is 8, learning rate is  $10^{-4}$ , the optimizer is ADAM with  $\epsilon = 10^{-8}$ , gradient clip is 0.5, and the  $L_2$ -regularizer coefficient is  $10^{-7}$ . The LSTM starts training after at least 32 trajectories have been collected from the environment. The replay buffer stores maximum of 128 trajectories of length 512.

## D.2. Additional Empirical Results

Figure 19 shows the learning curves of Meta-PWTD, A2C-RR, and the A2C baseline.



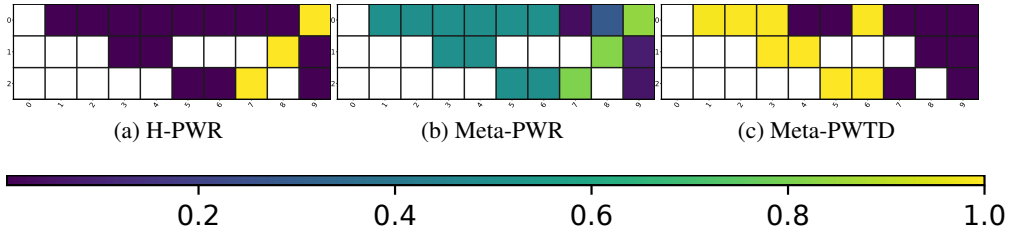


Figure 10. Handcrafted, meta-learned reward weights, and meta-learned TD-error weights in the depth 4 DAG environment in **a**, **b**, and **c** respectively. White is unreachable. Y-axis has been cropped to only include weights that affect inner loop learning.

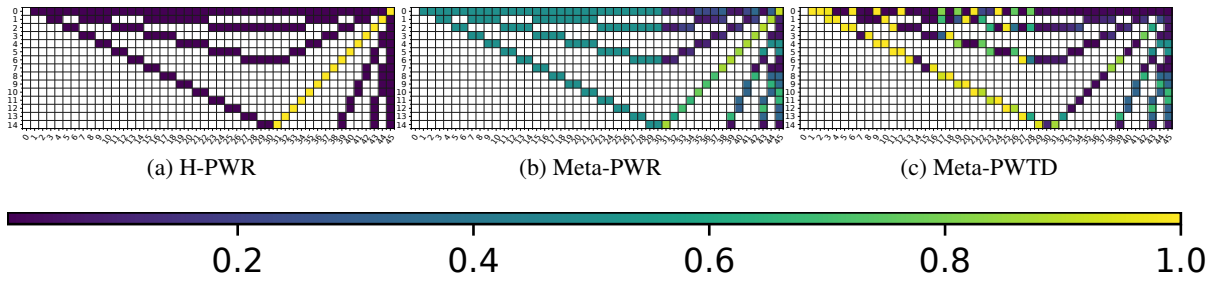
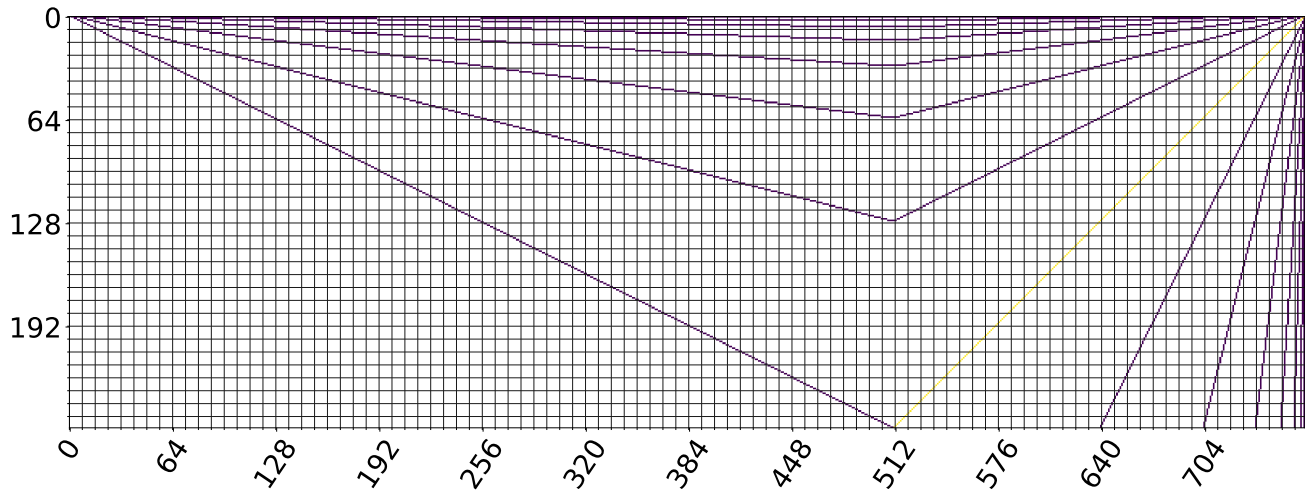
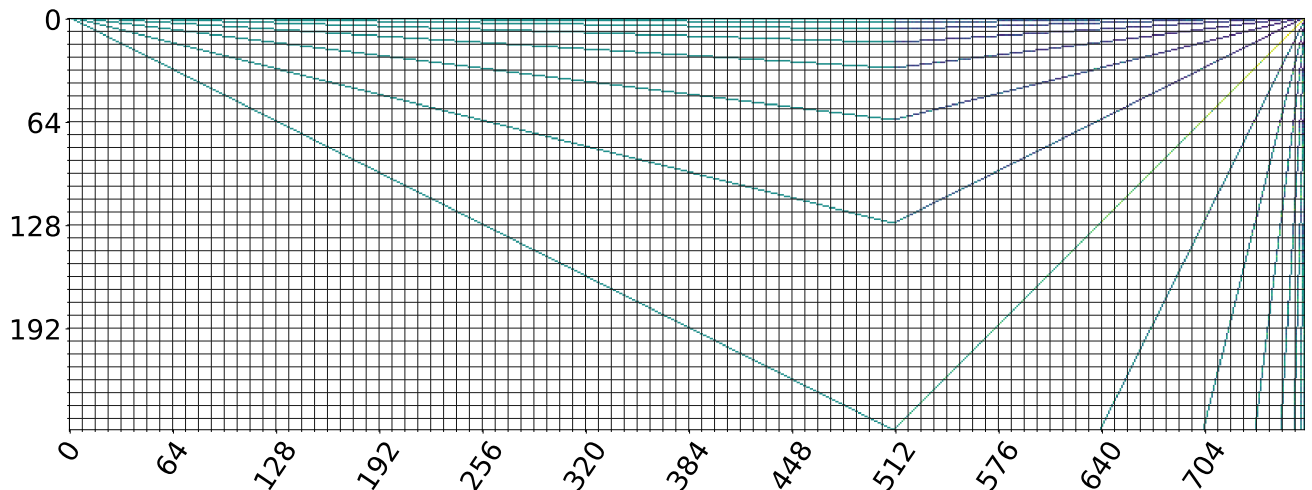


Figure 11. Handcrafted, meta-learned reward weights, and meta-learned TD-error weights in the depth 8 DAG environment in **a**, **b**, and **c** respectively. White is unreachable. Y-axis has been cropped to only include weights that affect inner loop learning.

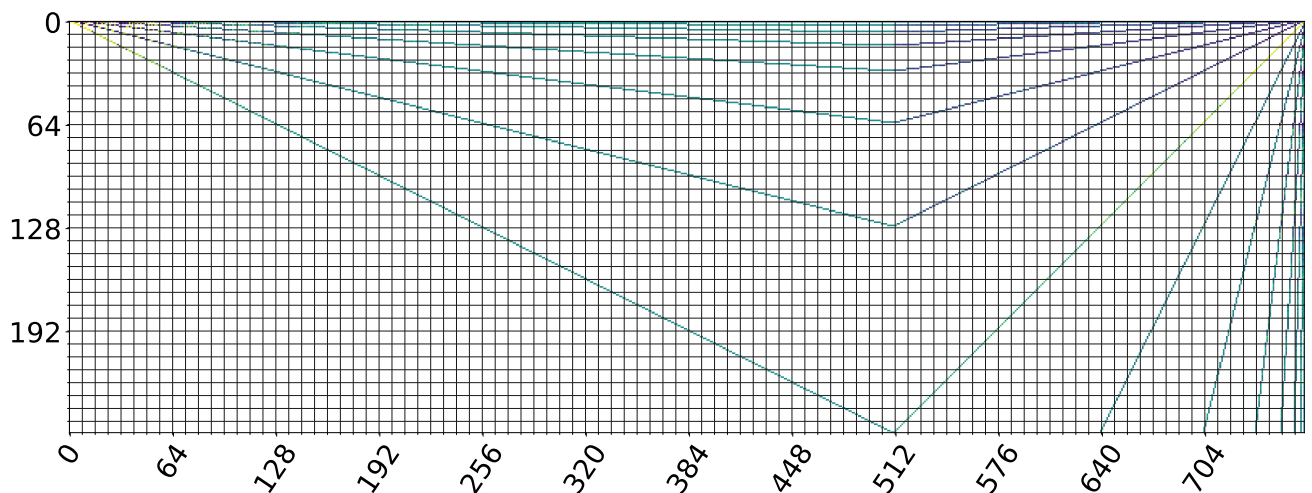
Pairwise Weights for Temporal Credit Assignment



(a) H-PWR



(b) Meta-PWR



(c) Meta-PWTD



Figure 12. Handcrafted, meta-learned reward weights, and meta-learned TD-error weights in the depth 16 DAG environment in **a**, **b**, and **c** respectively. White is unreachable. Y-axis has been cropped to only include weights that affect inner loop learning.

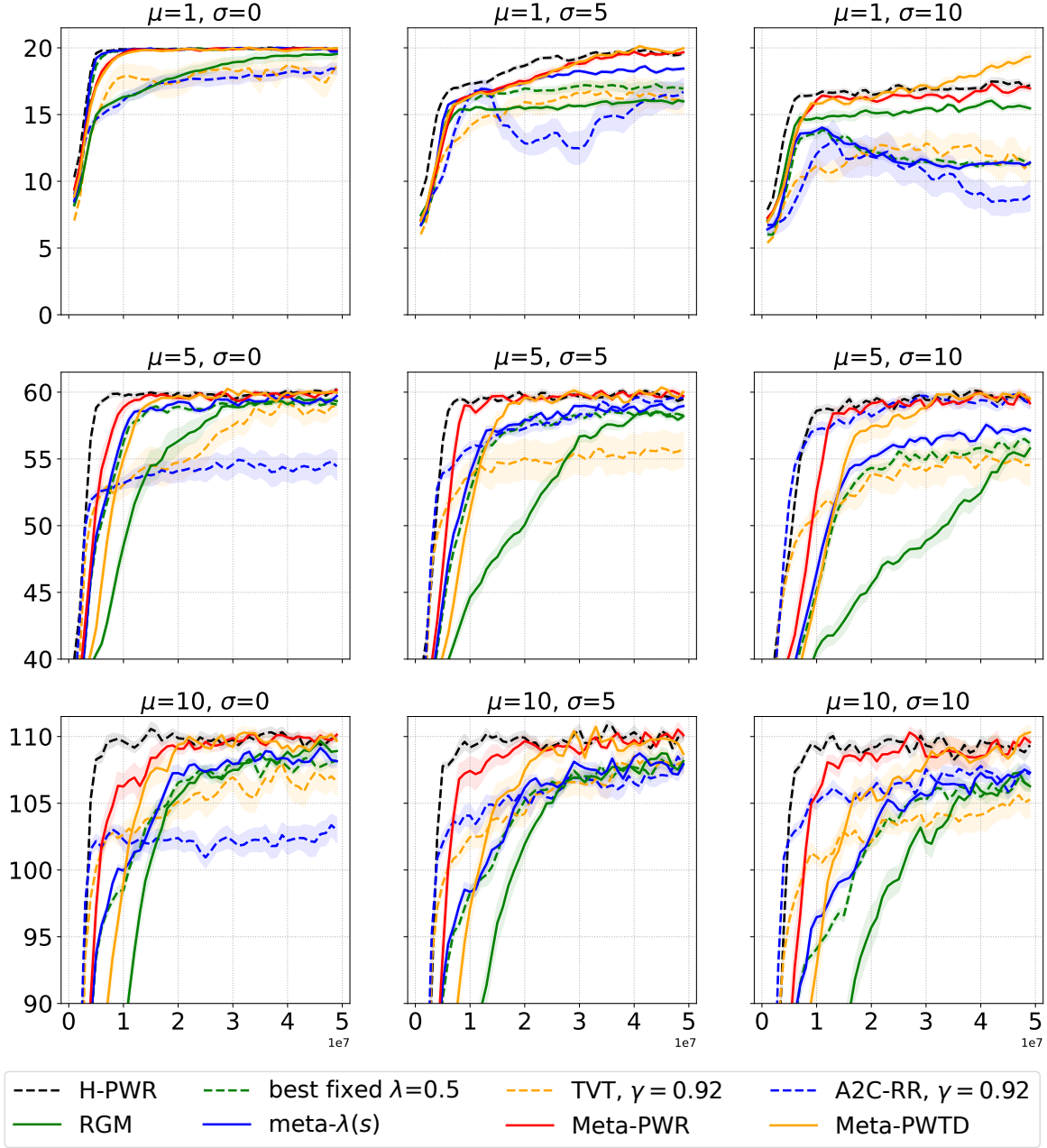


Figure 13. Episode returns in all 9 variants of the Key-to-Door environment. The x-axis is the number of frames. Rows are the different apple reward means ( $\mu$ ), columns the different apple reward variance ( $\sigma^2$ ). The x-axis reflects the number of frames, y-axis the episode return. The curves show the average over 10 independent runs with different random seeds and the shaded area shows the standard errors.

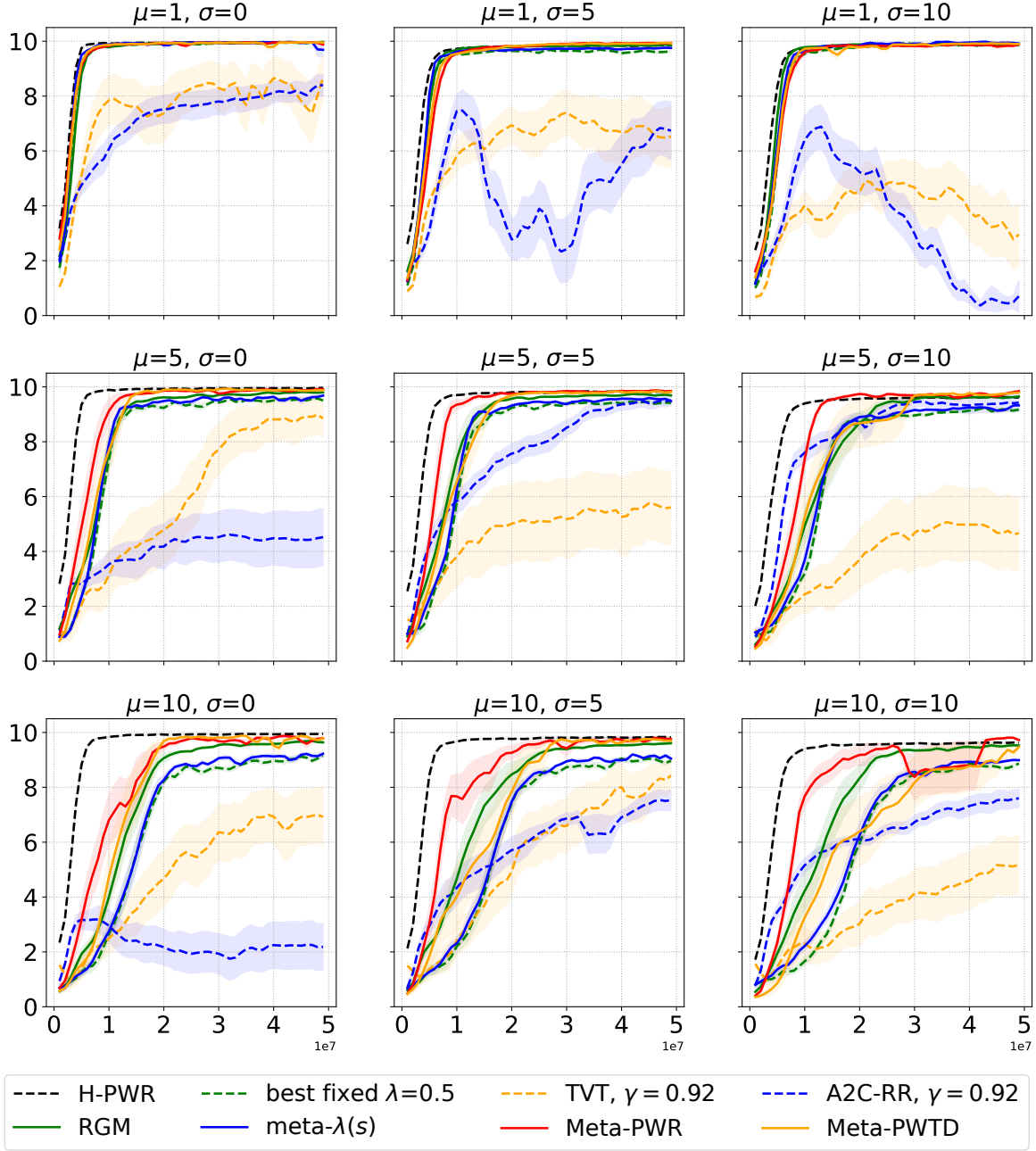


Figure 14. Door phase returns in all 9 variants of the Key-to-Door environment. The x-axis is the number of frames. Rows are the different apple reward means ( $\mu$ ), columns the different apple reward variance ( $\sigma^2$ ). The x-axis reflects the number of frames, y-axis the door phase return. The curves show the average over 10 independent runs with different random seeds and the shaded area shows the standard errors.



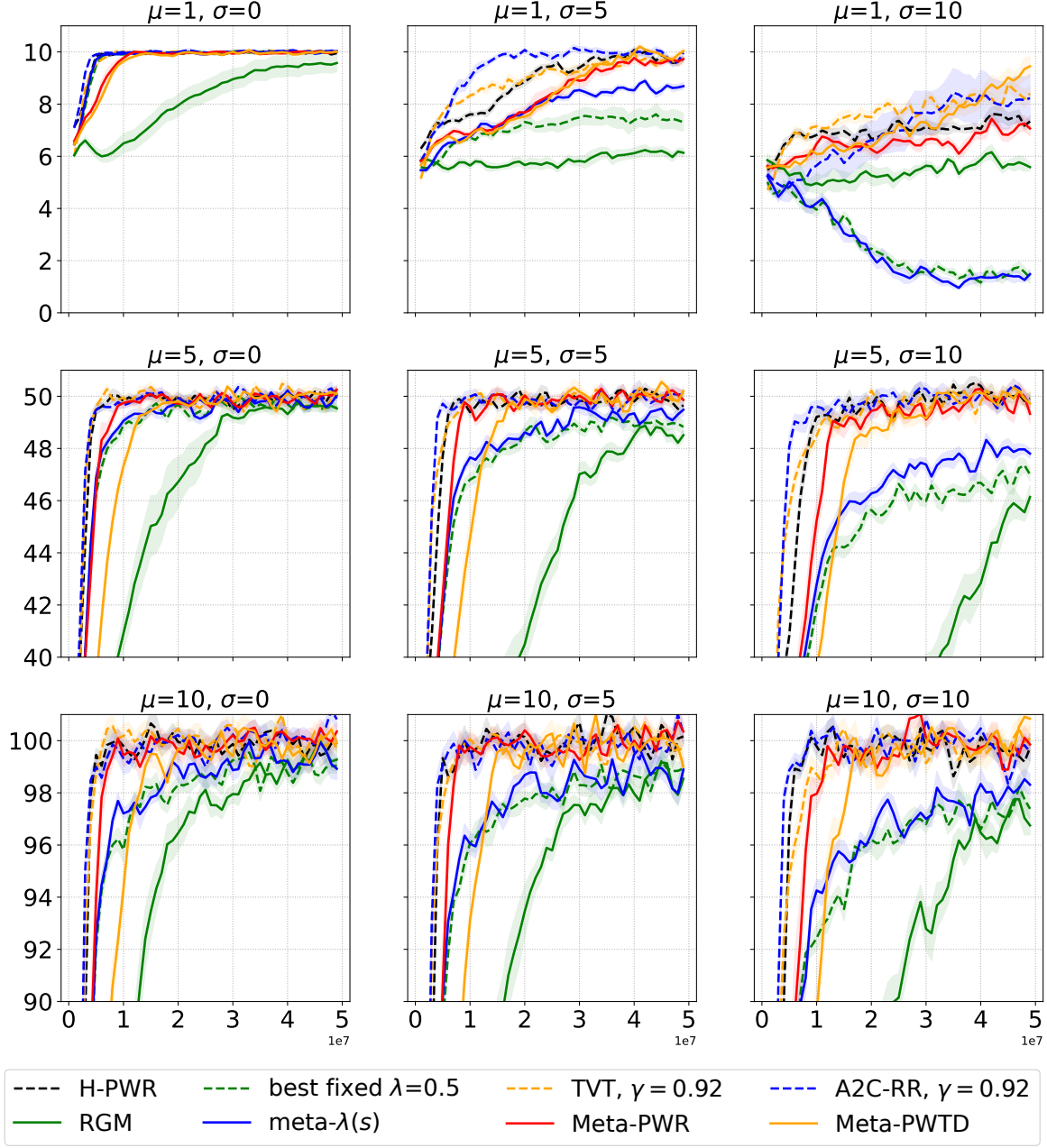


Figure 15. Apple phase returns in all 9 variants of the Key-to-Door environment. The x-axis is the number of frames. Rows are the different apple reward means ( $\mu$ ), columns the different apple reward variance ( $\sigma^2$ ). The x-axis reflects the number of frames, y-axis the apple phase return. The curves show the average over 10 independent runs with different random seeds and the shaded area shows the standard errors.

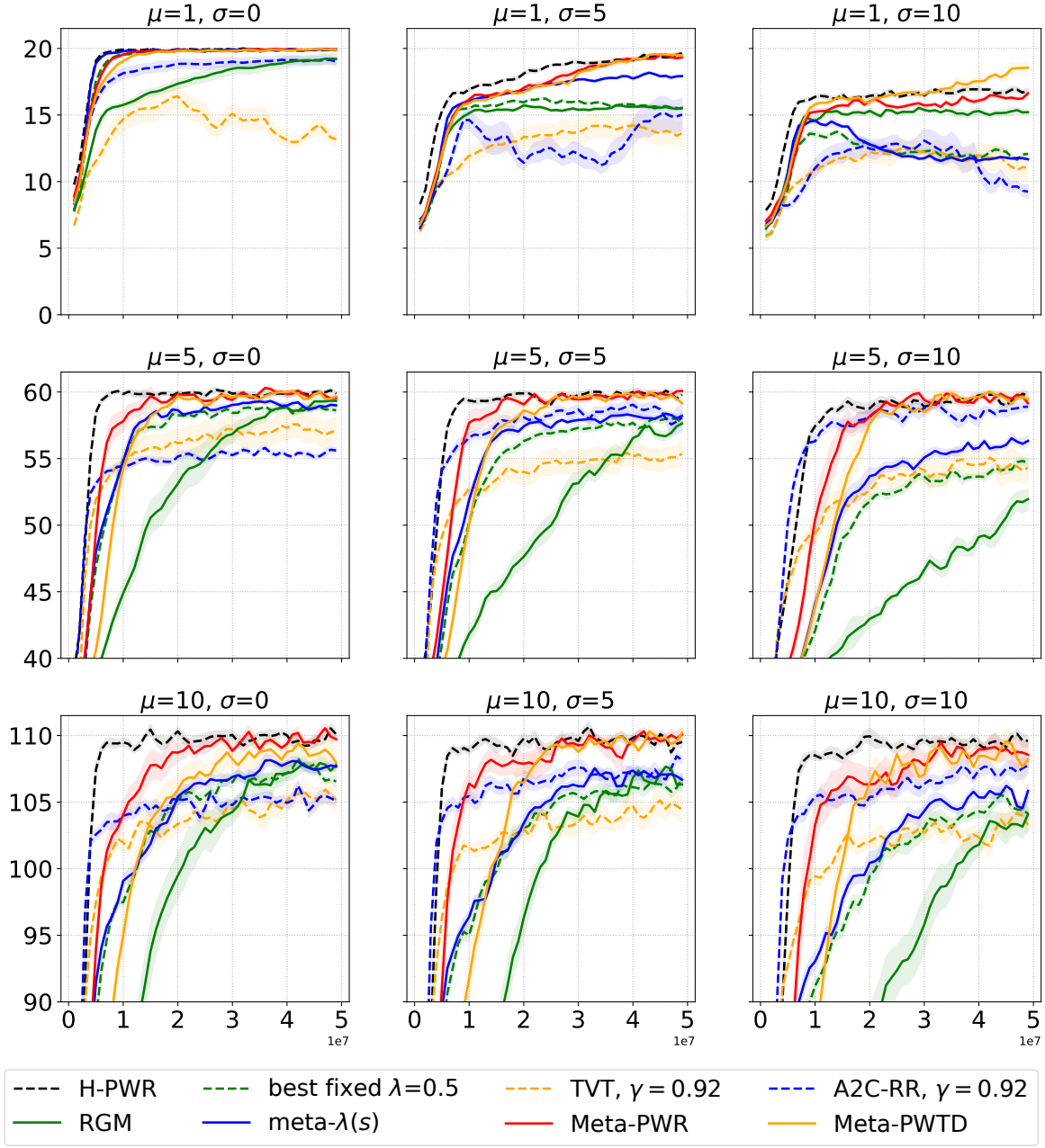


Figure 16. Episode returns in all 9 variants of the stochastic Key-to-Door environment. The x-axis is the number of frames. Rows are the different apple reward means ( $\mu$ ), columns the different apple reward variance ( $\sigma^2$ ). The x-axis reflects the number of frames, y-axis the episode return. The curves show the average over 10 independent runs with different random seeds and the shaded area shows the standard errors.

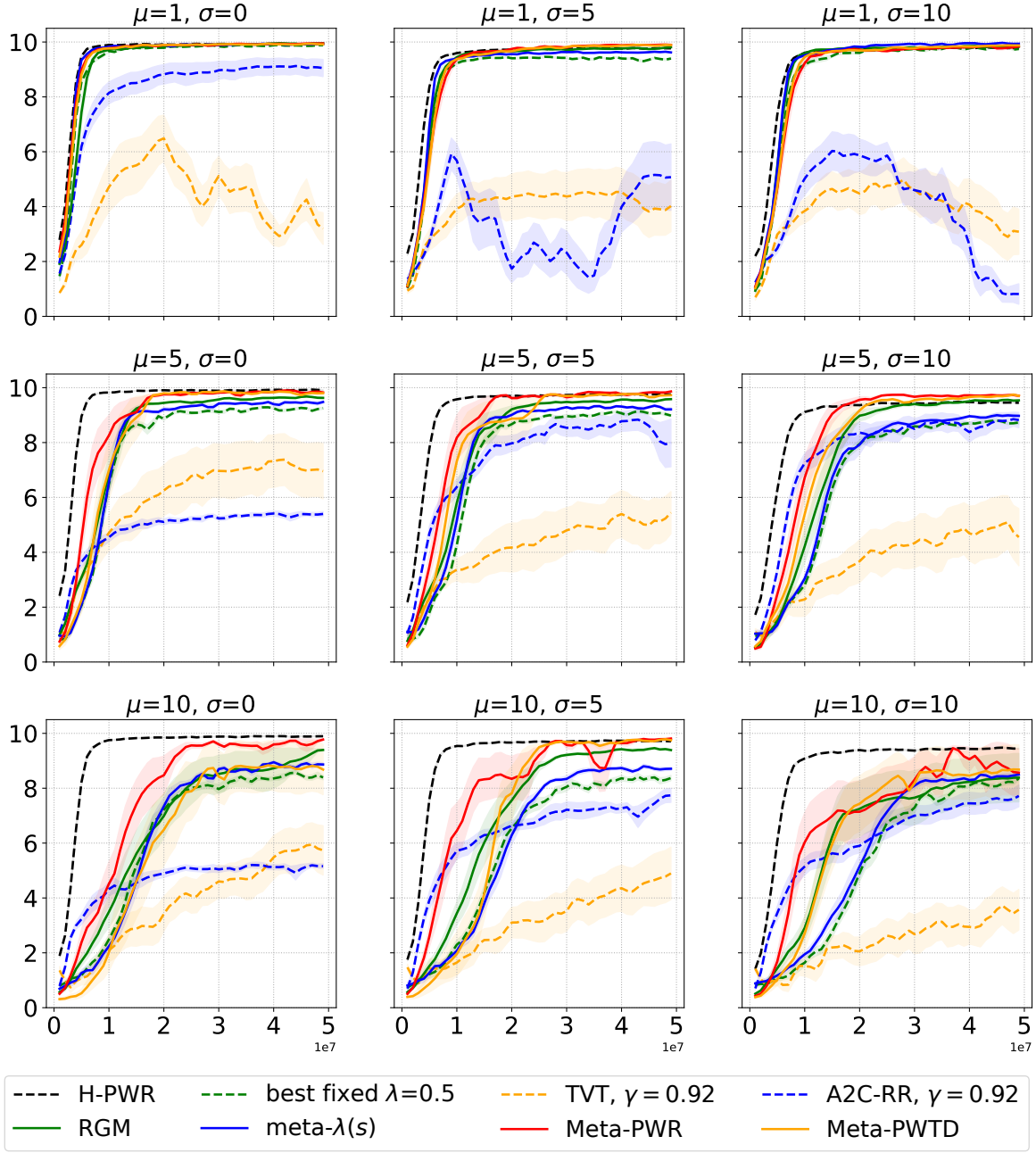


Figure 17. Door phase returns in all 9 variants of the stochastic Key-to-Door environment. The x-axis is the number of frames. Rows are the different apple reward means ( $\mu$ ), columns the different apple reward variance ( $\sigma^2$ ). The x-axis reflects the number of frames, y-axis the door phase return. The curves show the average over 10 independent runs with different random seeds and the shaded area shows the standard errors.

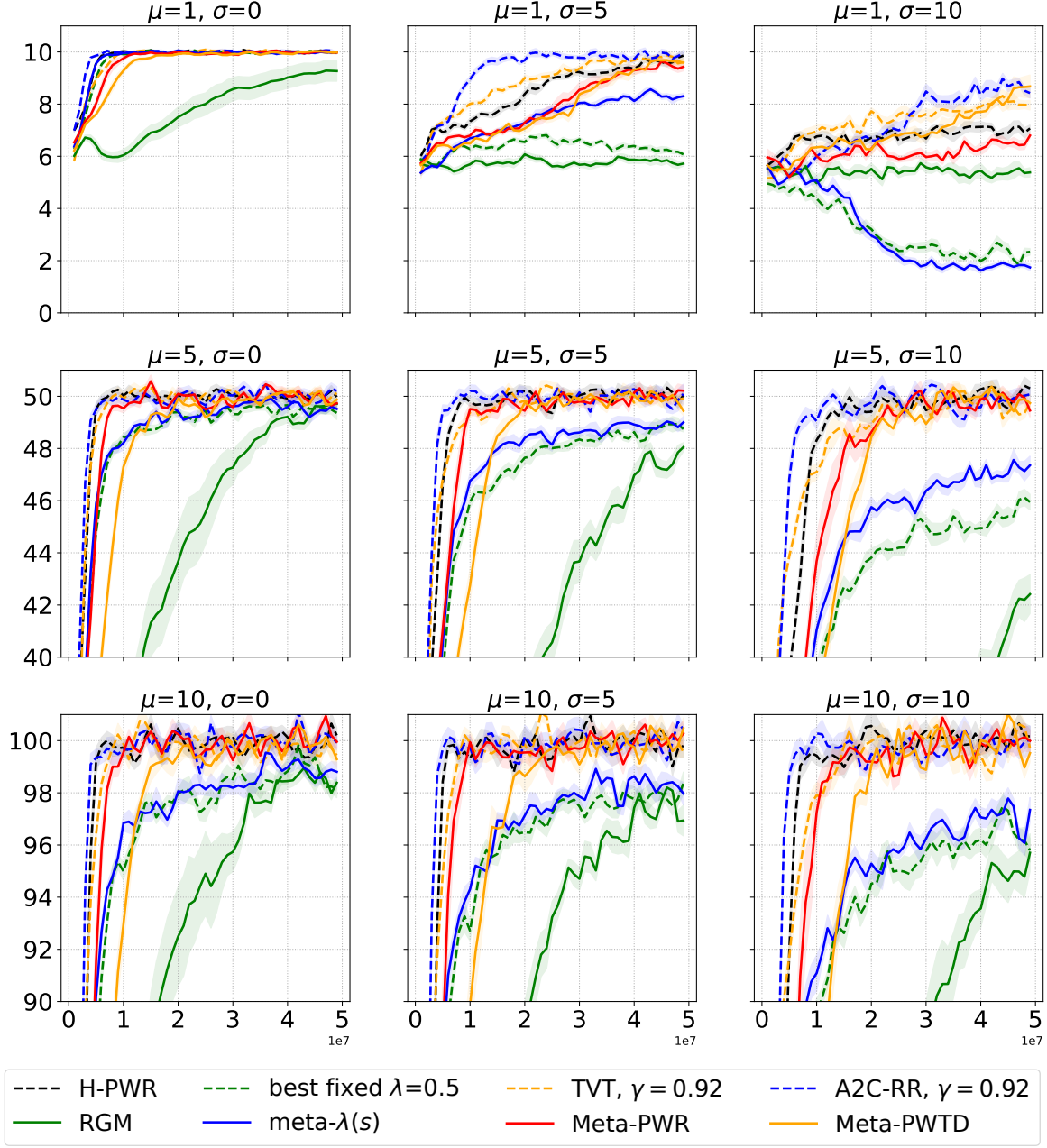


Figure 18. Apple phase returns in all 9 variants of the stochastic Key-to-Door environment. The x-axis is the number of frames. Rows are the different apple reward means ( $\mu$ ), columns the different apple reward variance ( $\sigma^2$ ). The x-axis reflects the number of frames, y-axis the apple phase return. The curves show the average over 10 independent runs with different random seeds and the shaded area shows the standard errors.

## Pairwise Weights for Temporal Credit Assignment

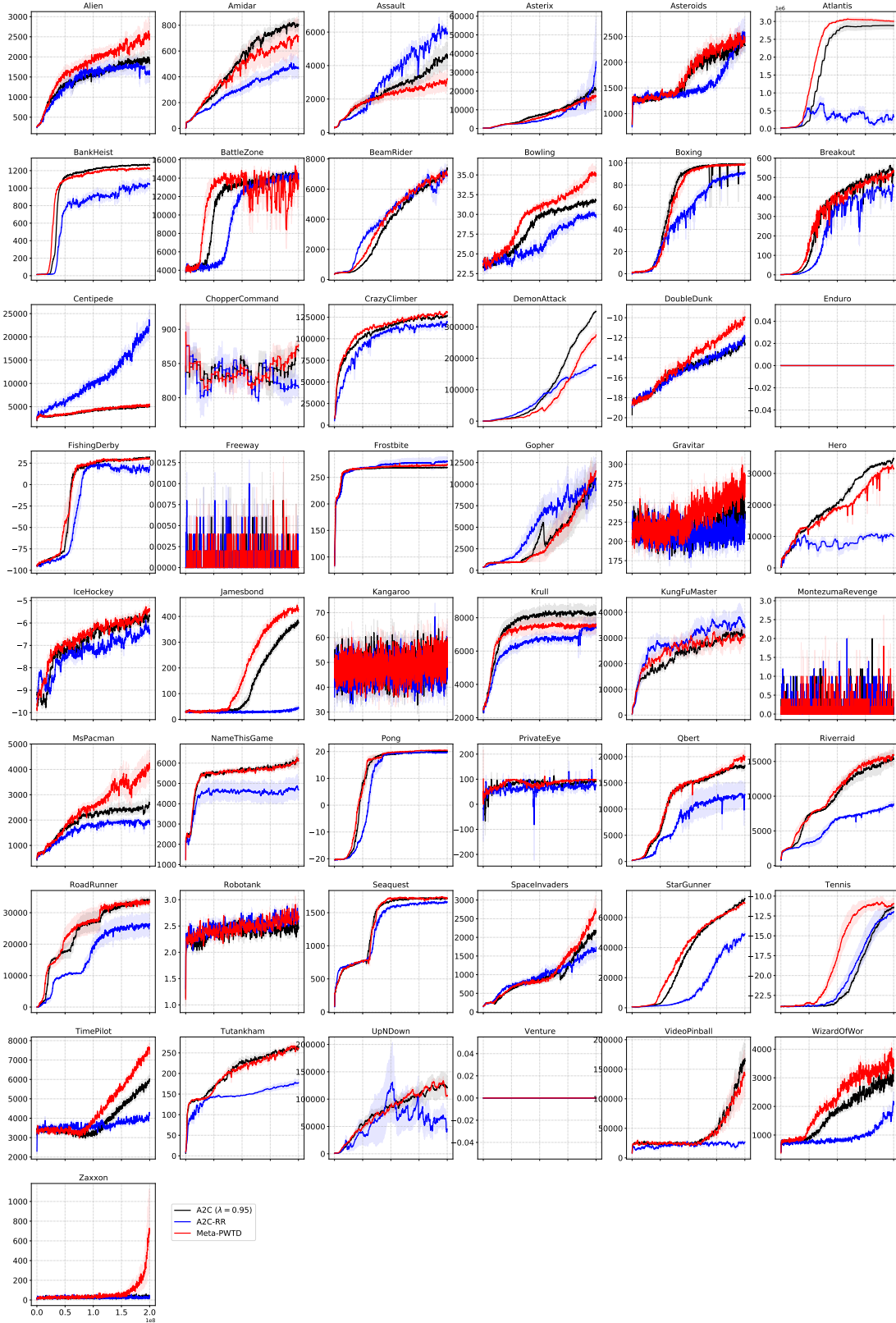


Figure 19. Learning curves on 49 Atari games. The x-axis is the number of frames and the y-axis is the episode return. Each curve is averaged over 5 independent runs with different random seeds. Shaded area shows the standard error over 5 runs.